EARTH NOISE IN THE 20- TO 100-SECOND PERIOD RANGE

E. J. Douze

Teledyne Geotech

Prepared for:

Air Force Office of Scientific Research

9 September 1975

SECURITY CLASSIFICATION OF THIS PAGE (When Data Entered)

REPORT DOCUMENTATION PAGE

READ INSTRUCTIONS BEFORE COMPLETING FORM

1. REPORT NUMBER: AFOSR - TR - 76 - 0376	2. GOVT ACCESSION NO.
3. RECIPIENT'S CATALOG NUMBER	
4. TITLE (and Subtitle): EARTH NOISE IN THE 20- TO 100-SECOND PERIOD RANGE, FINAL REPORT	5. TYPE OF REPORT & PERIOD COVERED: FINAL REPORT
6. PERFORMING ORG. REPORT NUMBER: TR 75-14	
7. AUTHOR(s): E. J. Douze	8. CONTRACT OR GRANT NUMBER(s): F44620-73-C-0052
9. PERFORMING ORGANIZATION NAME AND ADDRESS: Teledyne Industries, Inc., Geotech Division, 3401 Shiloh Road, Garland, Texas 75041	10. PROGRAM ELEMENT, PROJECT, TASK AREA & WORK UNIT NUMBERS: 62701E, AO 1827-19
11. CONTROLLING OFFICE NAME AND ADDRESS: Advanced Research Projects Agency/NMR, 1400 Wilson Blvd., Arlington, VIrginia 22209	12. REPORT DATE: 9 September 1975 13. NUMBER OF PAGES: 58
14. MONITORING AGENCY NAME & ADDRESS(if different from Controlling Office): Air Force Office of Scientific Research/NP, 1400 Wilson Boulevard, Arlington, Virginia 22209	15. SECURITY CLASS. (of this report): Unclassified 15a. DECLASSIFICATION/DOWNGRADING SCHEDULE

16. DISTRIBUTION STATEMENT (of this Report)

Approved for public release; distribution unlimited

17. DISTRIBUTION STATEMENT (of the abstract entered in Block 20, if different from Report)

18. SUPPLEMENTARY NOTES

TECH, OTHER

19. KEY WORDS (Continue on reverse side if necessary and identify by block number)

Long-Period Seismic Noise; Sources and Suppression

20. ABSTRACT (Continue on reverse side if necessary and identify by block number)

Experiments to investigate the sources of seismic noise in the period range of 20 to 100 seconds have been conducted at three observatories, Grand Saline and McKinney, Texas and Pinedale, Wyoming.

For surface seismographs the main contributor to the noise is quasi-static earth motion caused by wind-generated pressure variations. These pressure

DD FORM 1 JAN 73 1473 EDITION OF 1 NOV 65 IS OBSOLETE

UNCLASSIFIED

SECURITY CLASSIFICATION OF THIS PAGE (When Data Entered)

20. ABSTRACT, Continued

variations were recorded by microbarographs and shown to be linearly related to the noise recorded by seismographs during windy periods. During windless periods frequency-wave number analysis shows that infrasonic waves contribute to the noise recorded by long-period seismometers. Attenuation of the effect of short wavelength wind-generated pressure variations can be accomplished by two means: burial of the seismometer below the surface and optimum filtering techniques. The depth of burial required to eliminate the wind-generated noise is approximately in agreement with theory. At hard rock sites, such as granite, a depth of 50 m is sufficient to eliminate the noise entirely on the vertical seismographs and the horizontals are only affected during extreme windy periods.

The wind-generated noise on vertical seismographs can be suppressed by using least-mean-square filters that use the pressure variations recorded by a microbarograph to predict the noise recorded by the seismometer from the same source. It is usually possible to eliminate 70 to 90 percent of the increased noise level on vertical seismographs caused by the wind. For the horizontal seismographs the prediction is less effective because of the susceptibility to environmental effects of these tilt sensitive instruments.

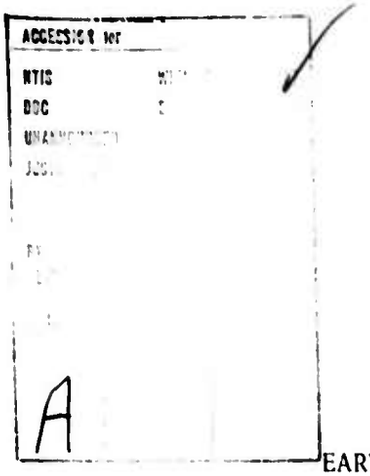

TECHNICAL REPORT NO. 75-14

EARTH NOISE IN THE 20- TO 100-SECOND PERIOD RANGE

FINAL REPORT

CONTRACT F44620-73-C-0052

by

E. J. Douze

TELEDYNE GEOTECH
3401 Shiloh Road
Garland, Texas

9 September 1975

CONTENTS

ILLUSTRATIONS

ILLUSTRATIONS, CONTINUED

ILLUSTRATIONS, Continued

EARTH NOISE IN THE 20- TO 100- SECOND PERIOD RANGE
FINAL REPORT
CONTRACT F44620-73-C-0052

1. INTRODUCTION

Quasi-static deformations in response to atmospheric pressure changes account for much of the ambient earth noise at periods greater than 20 seconds. While local variations in atmospheric pressure may arise from a variety of sources, only two appear to produce significant earth motion on a more or less continuous basis. These are the turbulent air flow associated with the surface wind (Sorrells et al., 1971, Ziolkowski, 1973) and naturally occurring infrasonic waves (Sorrells and Douze, 1974). The essential difference between these two phenomena, insofar as the earth is concerned, is that they occupy widely separated regions of the wave-number spectrum of the atmospheric pressure field. In the 20-100 second period range, the convective wavelengths associated with wind generated turbulence rarely exceed a kilometer and may be as small as several tens of meters. On the other hand, infrasonic pressure fluctuations in the same period range commonly have wavelengths which are of the order of several tens of kilometers. Since the quasi-static pressure response of the earth tends to increase monotonically as the wavelength of the pressure oscillation increases (Sorrells, 1971, Sorrells et al., 1971), infrasonic waves will, in general, cause much larger deformations than wind-generated atmospheric changes with the same power spectral density. At the surface, during windy intervals, this difference in responses is more than offset by the differences in the local pressure amplitudes of the two sources. Because of the differences in wavelengths, the earth's response to acoustic waves may exceed its response to wind related pressure changes by about a factor of 5-10. However, the amplitudes of wind related atmospheric pressure fluctuations can easily be 1-2 orders of magnitude greater than the amplitudes of infrasonic waves with the same period. Therefore, during intervals of moderately high wind speeds (>4 meters/sec) the pressure related earth noise recorded at or near the surface will be dominated by quasi-static deformations in response to wind-generated pressure changes. Both theoretical studies (Sorrells, 1971, Ziolkowski, 1973) and experimental studies (Sorrells et al., 1971) demonstarate that wind related earth noise can be vertually eliminated in the 20-100 second period range by installing the seismographs at depths on the order of several hundred meters.

An alternative method of reducing pressure related earth noise was also considered. It has been known for some time that during windy intervals there is a strong correlation between the outputs of colocated microbarographs and seismographs (Capon, 1969, Sorrells et al., 1971). Therefore, it is possible to estimate the pressure generated earth noise by applying an appropriate filter to the output of the microbarograph. Noise reduction is obtained by subtracting this estimate from the recorded seismogram.

Information collected from three experimental long-period installations will be used in this report. A brief description of each site follows:

a. McKinney, Texas; consisted of meteorological equipment and a surface seismological observatory, and was used principally to study the effect of wind-induced pressure variations on surface seismographs. The meteorological instrumentation consisted of 13 microbarographs and three anemometers; one microbarograph array of six instruments was closely grouped around the seismometer vault with average separations of around 1 km and included a microbarograph colocated with the seismograph vault. The remaining seven microbarographs, with separations of around 5 km between sensors constituted a second array, also available to study long-wavelength acoustic waves. Four microbarographs were installed for a limited time at a distance of 50 m from the vault to study wind-generated noise. The basic seismic instrumentation consisted of a pair of horizontal and a pair of vertical seismographs, Teledyne Geotech Model 7505A and Geotech solid-state amplifiers (Model 28450). These surface seismometers were enclosed within insulated, pressure-tight tank vaults which were mounted in the floor of a concrete bunker. The roof of the bunker was below ground level with access through a pressure-tight hatch. Data from all the sensors were recorded on a digital acquisition system described in detail by Herrin and McDonald (1971). In addition the data were recorded continuously on 16 mm film.

b. Grand Saline, Texas; experiments were performed at a salt mine owned by the Morton Salt Company. The seismic instrumentation consisted of two 3-component sets of long-period seismographs installed at the surface and in the mine. The mine seismographs were at a depth of 183 m below the surface and approximately 100 m of horizontal distance from the surface installation. One microbarograph was colocated with the surface system and one microbarograph was used to measure pressure variation inside the mine. The system is described in detail by Herrin and McDonald, 1971, and Sorrells et al., 1971.

Directly below the site the velocity structure is controlled by the salt dome. Approximately 90 m of sandy clay with interbedded sand lenses occur above the salt. Compressional wave velocities of 1.4 and 4.7 km/sec (Anderson and Lieberman, 1946) were used for the salt dome mode with a Poisson's Ratio of 0.33. The velocity structure of the sediment surrounding the salt dome were taken from a sonic log some 7 km from the site; the log shows gradual increase in compressional velocity from 1.4 km/sec at the surface to 6 km/sec at 3.6 km depth.

c. Pinedale, Wyoming; the site is located 30 km west of Pinedale, Wyoming; the surface instrumentation consisted of a set of surface seismographs in a vault approximately 8 m below the surface and a microbarograph located 15 m from the surface vault (Douze and Sherwin, 1975). In addition, two down-hole long-period KS seismograph systems were installed. The KS seismometer has not been described in the open literature, but a brief description of it was given by Starkey (1973). One was placed throughout the experiment in a shallow hole at a depth of 46 m. The other deep-hole instrument was operated at different depths in an adjacent 3000 m hole. Because of an obstruction in the casing at 1376 m, operation below this depth was not possible. The hole was filled with water below a depth of 190 m; as will be discussed later, the presence of liquid in the hole affected the performance of the seismometer. The data were

recorded on FM analog tape at sufficiently high levels so that tape noise was not a problem in the period range of 20 to 100 seconds. The velocity structure of the site is very simple; the deep hole was drilled in granite from a few feet below the surface to the total depth of 3050 m. A sonic and a density log were run and an almost constant velocity of 5.5 km/sec and density of 2.6 g/cm^3 were measured.

2. THEORY

Studies by Sorrells et al. (1971) and Savino et al. (1972) have demonstated that a significant portion of the seismic noise with frequencies lower than about 0.05 Hz is related to atmospheric pressure variations. For the purposes of discussion, it is convenient to separate the atmospheric pressure field into wind-generated and wind-free components. Savino et al. (1972) were concerned with the earth motion in response to wind-free pressure changes. In contrast, our work (Sorrells, 1971; Sorrells et al., 1971; and Sorrells and Goforth, 1973) has been concerned primarily with wind-related earth noise.

In order to account for the observed earth motion, it is necessary to make certain assumptions about the statistical properties of the pressure field and the distribution of elastic constants within the earth. We originally assumed that the wind-generated pressure field could be approximated by a wave which was convected at a speed equivalent to the mean wind speed. This assumption was based upon Taylor's Hypothesis (Lumley and Panofsky, 1964) which states in effect that, if the turbulent velocity fluctuations are small compared to the main stream velocity, the time variations in the pressure, as observed at a fixed point in the flow, would be approximately the same as that due to the convection of an unchanging spatial pattern past the point with the mean flow velocity. In addition, we initially assumed that the earth could be approximated by a perfectly elastic, homogeneous half-space. Later experimental work (Sorrells et al., 1971) demonstrated the need for a more precise description of the shallow distribution of elastic constants; therefore, a model was adopted which consisted of isotropic, elastic layers separated by parallel boundaries. A somewhat surprising outcome of that particular study was that once the layered earth model was adopted, relatively good agreement was obtained between theory and experiment, despite the fact that a plane wave is a gross oversimplification of the structure of the wind-generated atmospheric pressure field. Sorrells and Goforth (1973) expanded the theory to cover the case where the pressure field is a random process which is stationary in time and homogeneous in space. In particular, they derived expressions for the transfer function and the coherence which relate earth motion to pressure changes observed at a point on the earth's surface. They represented the spatial organization of the wind-generated pressure field as scattered waves traveling at speeds varying from $c = \omega/(\zeta+\rho)$ to $c = \omega/(\zeta-\rho)$ and arriving from directions which vary from $-\Psi$ to Ψ, where ζ is the midpoint and $(\zeta\pm\rho)$ the extrema of the wave-number range of interest. For a distributed source of

this type, and for pressure convection velocities small compared to seismic velocities, the resultant vertical displacement and apparent horizontal displacement are given by

$$V(\omega) = \frac{1}{4\rho\Psi\zeta} \int_{-\Psi}^{\Psi} \int_{\zeta-\rho}^{\zeta+\rho} G_v(k)\, k\, dk\, d\theta \qquad (1)$$

and

$$H(\beta,\omega) = \frac{1}{4\rho\Psi\zeta} \int_{-\Psi}^{\Psi} \int_{\zeta-\rho}^{\zeta+\rho} \cos(\theta-\beta) \left[G_r(k) - \frac{igk}{\omega^2} G_v(k)\right] k\, dk\, d\theta \qquad (2)$$

where

$G_v(k)$ is the vertical component of the earth's response to a point pressure load

$G_r(k)$ is the radial component (including tilt) of the earth's response to a point pressure load

k is the wave number which is determined by specifying the frequency, ω, and the convection velocity, c, of the pressure wave

β is the direction in which the tilts are observed

g is the acceleration due to gravity

Sorrells and Goforth (1973) found that the above transfer functions, which are based on an analytical model possessing all of the observable properties of the wind-generated pressure field, are experimentally indistinguishable from those associated with a plane pressure wave. The analagous, but simpler, transfer functions for a plane wave are

$$V(\omega) = G_v\left(\frac{\omega}{c}\right) \qquad (3)$$

$$H(\beta, \omega) = \cos(\eta-\beta) \left[G_r\left(\frac{\omega}{c}\right) - \frac{ig}{\omega c} G_v\left(\frac{\omega}{c}\right)\right] \qquad (4)$$

where

$G_v\left(\frac{\omega}{c}\right)$ is the vertical component of the earth's response to a plane pressure wave of frequency ω and velocity c

$G_r\left(\frac{\omega}{c}\right)$ is the radial component of the earth's response to a plane pressure wave of frequency ω and velocity c

η direction of propagation of the plane wave

β direction in which the tilt is observed

The plane wave formulations were used to compute the theoretical spectra presented in this report.

3. ANALYSIS TECHNIQUES

In this section we briefly discuss the data processing methods used in this study; none of them are new and the only objective is to show how they were employed for the particular problems associated with eliminating pressure-generated noise. Appropriate references are cited for those interested in the details of any of the methods.

The basic inputs required are auto- and cross-correlation of the noise recorded by the seismograph and microbarographs: although these may be computed directly, the use of the Fast Fourier Transform (Cooley and Tukey, 1965) provides a more effective approach. The digital time series $t_m(k)$ is divided into M segments of K data points; each segment is transformed into the frequency domain

$$S_m(f) = \sum_{k=0}^{K-1} t_m(k) \exp\left\{\frac{-2\pi i f k}{K}\right\} \tag{5}$$

The spectral estimates are then obtained by averaging over a number of segments (M)

$$\hat{P}_{mn}(f) = \frac{1}{M} \sum_{j=1}^{M} S_{mj}(f) \cdot S^*_{nj}(f) \tag{6}$$

The $\hat{P}_{mm}$ are estimates of the spectra of the multiple time series and $\hat{P}_{mn}$ are the cross spectra. The asterisk indicates complex conjugate. This approach to the computation of power spectra was discussed in detail by Welch (1967).

At this point it is possible (Burg, 1964) to compute optimum filters directly in the frequency domain. For reasons that will be apparent later, we prefer to use the inverse Fourier Transform in the results of equation (6) and thus obtain the auto- and cross-correlations of the time series.

The optimum filters used have been described (see Robinson, 1967); we will only briefly summarize their applicability for the purpose of this study. Suppose we have N input microbarographs y_i (t), i = 1, N and we wish to predict the amount of energy on an output channel, x(t), the earth noise on the seismograph that is caused by the pressure variations recorded by the microbarographs. We desire a set of N filters, f(t) of length T, that can be applied to the N microbarographs to obtain an output z(t) that will closely approximate the desired output channel x(t).

$$z(t) = \sum_{i=1}^{N} \sum_{s=0}^{L} f_i(s) \cdot y_i(t-s) \qquad \begin{matrix} s = 0, L \\ t = 0, T + L + 1 \end{matrix} \tag{7}$$

We seek the filters by minimizing the error function defined as

$$E = \sum_{t=0}^{T+L+1} \left[\sum_{i=1}^{N} \sum_{s=0}^{L} f_i(s)\, y_i(t-s) - x(t) \right]^2 \tag{8}$$

The error E is minimized when the partial derivatives with respect to the filter coefficients are put equal to zero

$$\partial E / \partial f_k\ (s) = 0 \text{ for } k = 1, N;\ s = 0, L.$$

The derivation is straightforward (Robinson, 1967) and results in:

$$\sum_{i=1}^{N} \sum_{s=0}^{L} R_{ki}\ (u-s)\ f_i(s) = C_k(u) \tag{9}$$

where R_{ki} is the multichannel correlation matrix of the inputs, the microbarograph channels we are using, and the C_k are the cross-correlations between the desired output, the seismograph, and the microbarographs.

Examination of the equation (9) shows that it consists of a large number of simultaneous equations. Fortunately, there is available an effective recursive method of solving for the desired filters; e.g., we start by computing N 1-point filters and from them compute a 2-point filter, and so forth. The recursive approach, first described by Levinson (1949), is made possible by

the fact that the autocorrelation matrix is a Toeplitz matrix. The advantage of the approach is that at each reiteration the remaining error is computed and the effectiveness of that length of filter is known. Uusally the error will decrease rapidly and then level off, thus one finds the least number of filter points required. When processing large amounts of data, the savings in processing can become appreciable.

When processing data off-line, one is not confined to realizable filters (i.e., using only past values) but can also use future data points. In some cases the capability of the optimum filters is greatly improved by using non-realizable filters. However, because of the phase delays involved between the seismograph and microbarograph traces, no improvement is obtained by this procedure for the case under study here.

By means of coherence measurements it is possible to obtain an estimate of the fraction of the power that can be predicted. The ordinary coherence function (or coherence squared) is obtained from the auto- and cross-power spectra in the usual fashion

$$\gamma^2_{mn} = \frac{| P_{mn}(f) |^2}{P_{mm}(f)\ P_{nn}(f)} \tag{10}$$

It is a measure, frequency by frequency, of how much of the power on a seismograph trace can be predicted from the microbarograph input.

In the same fashion, the multiple coherence (Bendat and Piersol, 1966) can be used for the multichannel case; it is defined from the spectral matrix $\phi(f)$ of all the traces

$$\alpha^2_j = 1 - \frac{1}{\phi_{jj}(f)\ \phi^{jj}(f)} \tag{11}$$

$\phi_{jj}(f)$ = power spectrum of the j^{th} trace, the seismograph

$\phi^{jj}(f)$ = j^{th} diagonal element of the inverse of the spectral matrix.

The multiple coherence is a measure of the linear relationship between an output, in this case seismograph, and a number of inputs, the microbarographs. As such, it is a measure of how well a multichannel filter would be able to predict the noise recorded by the seismograph. As it is more economical to compute, we have used it extensively instead of actually computing the multi-channel filter and applying it to the data. One problem with the multiple coherence is the rapid increase of the bias in the estimate with increasing number of inputs for low coherences (White, 1973).

Extensive use was made of frequency-wave number spectra in order to study the structure of atmospheric pressure variations. Our method for making these estimates is an adaptation of an efficient computational algorithm described by Smart and Flinn (1971). The basic change was to extend the block averaging technique (Welch, 1967) to the estimation of frequency wave-number spectra. Briefly, suppose that $F_{j\ell}(\omega)$ is the finite Fourier transform of the ℓ^{th} time segment recorded by the j^{th} detector. It may be written as

$$F_{j\ell}(\omega) = A_{j\ell}(\omega) \{\exp[-i\alpha_{j\ell}(\omega)]\} \tag{12}$$

The power spectral and cross-power spectral density estimates are then given by

$$S_{jm}(\omega) = \frac{1}{L} \sum_{\ell=1}^{L} F_{j\ell}(\omega) F^{*}_{m\ell}(\omega) \tag{13}$$

where * denotes complex conjugation. Equation (13) yields power spectral density estimates for $m = j$ and cross-power spectral density estimates for $m \neq j$.

The frequency wave-number spectral estimate is defined as

$$P(\omega,k) = \sum_{j=1}^{V} \sum_{m=1}^{V} S_{jm}(\omega) \exp[ik \cdot (r_j - r_m)] \tag{14}$$

where r_j is the vector distance to the jth detector with reference to an arbitrary origin. Then through the use of equations (12) and (13) (Sorrells and Douze, 1974)

$$P(\omega,k) = \frac{1}{L} \sum_{\ell=1}^{L} \left| \sum_{j=1}^{N} A_{j\ell}(\omega) \exp(-i\alpha_{j\ell}(\omega) + ik \cdot r_j \right|^2 \tag{15}$$

Basically, (15) indicates that the f-k estimates for each time segment can be added. The Smart and Flinn algorithm is used to obtain these estimates and the Fisher statistic is computed (Smart and Flinn, 1971) in order to assign statistical significance to the results.

4. SOURCES OF SEISMIC NOISE IN THE 20-100 SECOND PERIOD RANGE

The noise recorded by a long-period seismograph can be broadly classified as either earth noise or "system" noise. Earth noise is the result of ambient vibrations of the ground regardless of whether the cause is elastic waves or quasi-static deformations caused by pressure variations in the atmosphere. "System" noise is used in this report both for the noise generated in the seismograph system and the noise within the immediate environment, principally the vault. The noise from the immediate environment is difficult to separate from other sources: effects such as buoyancy (Crary and Ewing, 1952), convection currents in casing or vault or bending of base plates (Holcomb, 1975), can all contribute to the environmental noise and are especially severe on surface horizontal seismcgraphs.

The system noise caused by the seismograph system is better known. Magnification at which long-period seismographs are presently operated is such that the noise from thermal agitation approaches the earth noise. A number of authors have investigated theoretical and experimental noise levels. Almost all experimental data are for standard mass-spring systems; the system noise of a force-balance seismograph (KD seismometer) is more difficult to determine because the usual method of replacing the mass with an equivalent resistor is not applicable.

Theoretical system noise levels have been recently discussed in detail by Fix (1972) and Melton (1975). Experimental results have been shown by Fix (1972), and Savino (1971) for conventional seismographs and by Douze and Starkey (1973) for the force-balance system used at Pinedale. In all cases the system noise is sufficiently low not to seriously affect the experimental results; however, it represents an appreciable percentage of the total noise recorded. Furthermore, it should be noted that system noise levels are almost always measured after careful maintenance of the system, and that the system noise may be appreciably higher under more normal operating conditions.

The background noise at periods greater than 20 seconds is quite stable as compared to the microseismic peaks which vary up to two orders of magnitude. Spectral estimates of the noise recorded in the 20-100 second period range by the vertical seismographs are shown in figure 1. The data from which these estimates were made were taken during calm intervals in the month of January 1974, at McKinney, Texas. Observe that the spread of the estimates is about 3 dB. The anticipated spread of estimates at the 90 percent confidence level for a time stationary process is 2.8 dB. Thus, these results imply that in the absence of wind-generated earth motion, the vertical seismic noise may be considered to be time stationary for intervals of time at least on the order of a month. These results are consistent with observations reported by Savino et al. (1972) regarding the spectra of seismic noise observed in the Ogdensburg mine at a depth of 542 meters. Agreement in this area is to be expected since the spectra observed at depths in excess of several hundred meters should be free of wind related earth noise most of the time. There is also some evidence which suggests that the calm interval vertical seismic noise spectrum may vary slightly from winter to summer at McKinney, Texas, as seen when the mean of the January 1974 estimates is compared to the estimates of September 1973.

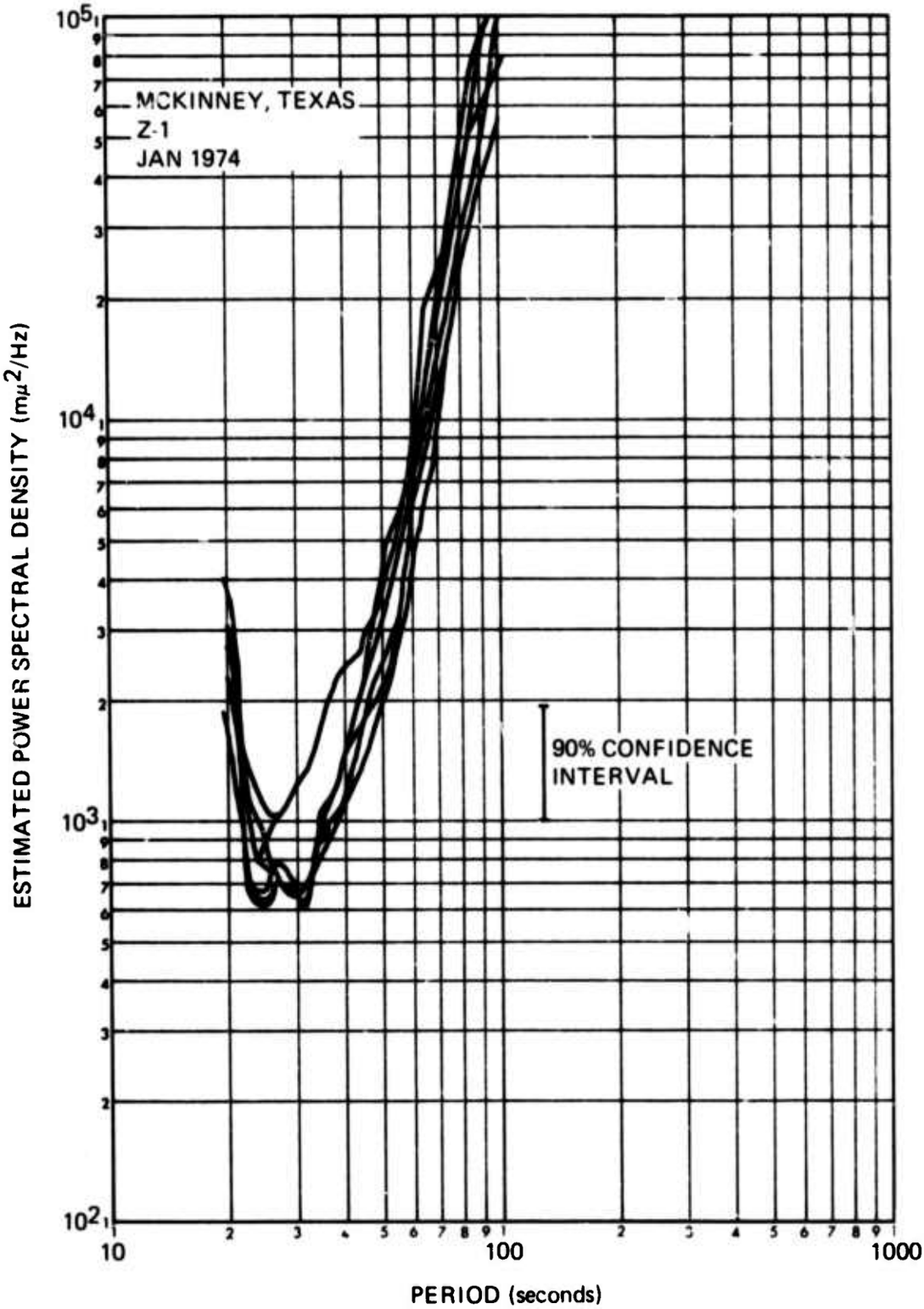

Figure 1. A comparison of noise power spectral densities. Data were recorded by a vertical seismograph during intervals when the mean wind speed was less than 1 m/sec. Spectral estimates have been corrected for system response, McKinney, Texas.

G 7569

The September 1973 estimate is about 3 dB lower than the January mean. This result suggests that the 10 dB seasonal variation in spectral amplitudes observed by Savino et al. (1972) is strongly suppressed at the McKinney site. On the other hand, the results at Pinedale, Wyoming varied approximately 10 dB over any month during the course of the experiment, June through December 1974.

Considering the numerous noise sources, i.e., system and environmental, it is often difficult to determine what is truly "earth noise." If we define earth noise as that portion of the noise that is coherent over distances of the dimension of the vault, an estimate of earth noise can be obtained by operating two seismographs in close proximity. The ratio of earth noise to other noise sources can be calculated from the power spectral density estimate and the coherence estimates between the outputs of the two seismographs. Under the appropriate experimental conditions the coherent power can be attributed to earth noise and the incoherent power to system noise. Let ρ_1 and ρ_2 denote the ESR (earth/system noise ratio) for each of the two seismographs and let γ_{12}^2 represent the square of the coherence between their outputs. Then it can be shown that,

$$\gamma_{12}^2 = \frac{\rho_1}{1 + \rho_1} \cdot \frac{\rho_2}{1 + \rho_2} \tag{16}$$

(e.g. Foster and Guinzy, 1967)

The ratio of power spectra R_{12}^2 can also be written in terms of ρ_1 and ρ_2, being given by,

$$R_{12}^2 = \frac{1 + \rho_1}{\rho_1} \cdot \frac{\rho_2}{1 + \rho_2} \tag{17}$$

Equations (16) and (17) may be solved for ρ_1 and ρ_2 yielding

$$\rho_1 = \frac{\gamma_{12}}{R_{12} - \gamma_{12}}$$

$$\rho_2 = \frac{\gamma_{12}}{\frac{1}{R_{12}} - \gamma_{12}} \tag{18}$$

For the surface vertical seismographs at McKinney it has been found that $\rho_1 \approx \rho_2$. Typical values estimated from calm interval samples are shown in figure 2. For reference, we have also included values of the ratio estimated for the vertical seismograph in the mine at Grand Saline, Texas, (Sorrells et al., 1971). It will be observed that at periods greater than about 50 seconds the ratios at McKinney are lower than those at Grand Saline. The cause of this discrepancy is not clearly understood at the present time. It appears to be related to a difference in the amplifiers used at the two locations. A phototube amplifier with a 30-second galvanometer was used at Grand Saline. A solid-state amplifier, instead of a phototube amplifier, is being used at McKinney. The lower ESR values found during our current program do

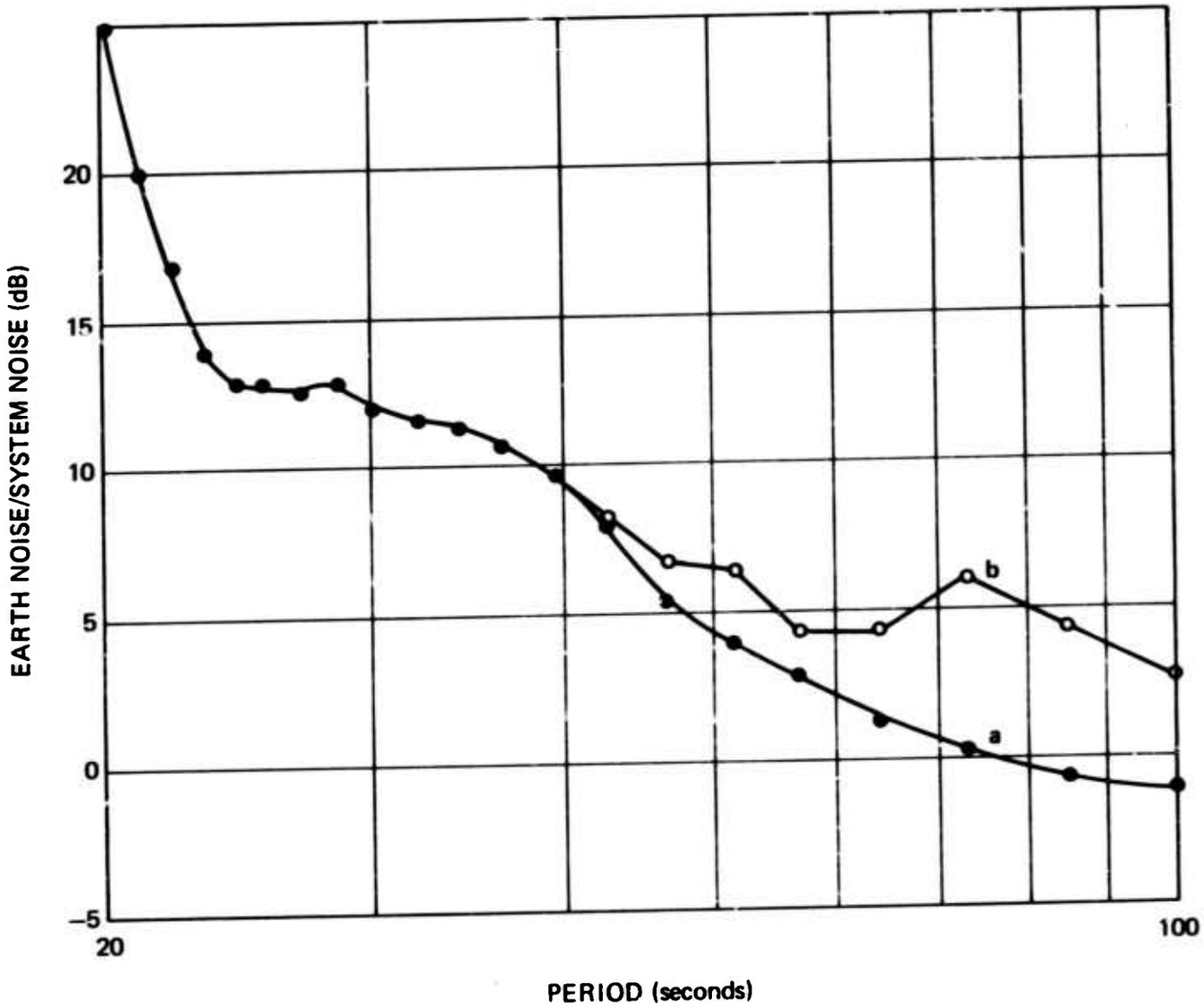

Figure 2. A representative estimate of the earth/system noise ratio for the vertical seismograph outputs (a) surface, McKinney, Texas, and (b) mine, Grand Saline, Texas.

G 7571

not seriously influence the outcome of our investigation. They do, however, limit the resolution with which pressure related earth motion can be separated from the noise generated by other sources, particularly at periods greater than 60 seconds.

During windless periods at McKinney, frequency-wave number spectra often show significant peaks (from the Fisher statistic) at high velocities. Because the microbarograph array used is small, it is difficult to determine whether the peaks are associated only with infrasonic waves traveling at 330 m/sec. An example of significant energy traveling at infrasonic velocities is shown in figure 3. However, a significant number of f-k spectra show even higher velocities such as shown in figure 4. The origin of these high-velocity pressure variations is not understood but they occur at levels sufficiently high to be recorded by the seismographs. The RMS amplitude range of these pressure changes is generally 0.1 to 5 μbars. At soft rock sites in the period range pressure variations of this order can be caused by winds with mean velocities as low as 0.5 m/sec.

In the f-k analysis the presence of wind noise rapidly decorrelating with distance has the same effect as adding white noise to the spectrum and the coherence between a single microbarograph and a seismograph will be significantly decreased. The reason for this is that the square of the ordinary coherence is a measure of the seismic noise power that is linearly predictable from a single microbarograph. However, as a general rule, not all of the pressure related earth noise recorded by a seismograph is predictable from the output of a co-located microbarograph. The sole exception occurs when variations in the atmosphereic pressure are the result of a plane wave (Sorrells and Goforth, 1973). As the structure of the pressure variations depart from this simple form the percentage of predictable earth noise will decline even though the total pressure contribution may remain constant. For this reason, it is sometimes necessary to resort to multiple coherence estimates to detect the presence of a pressure related component. In our case, the square of the multiple coherence is a measure of the percentage of the seismic noise power that is predictable from the outputs of an array of microbarographs. In the case of poorly organized pressure fields, the percentage of power predictable from a microbarograph array should be a better approximation to the total pressure related seismic noise power than that obtained from the ordinary coherence. However, in the case of well organized fields, ordinary and multiple coherence estimates should coincide and should be equal to the percentage of seismic noise power that is caused by atmospheric pressure variations.

One of the more interesting results of our investigations to date is that close agreement between ordinary and multiple coherence estimates is not uncommon. Examples calculated from data recorded during a calm interval on 29 January 1974, are shown in figure 5. Frequency wave-number estimates of variations in the atmospheric pressure field for the same interval yielded somewhat ambiguous results because of the relatively small aperture of the microbarograph array. There is, however, some suggestion that infrasonic waves are the principal source of atmospheric pressure variations during this interval. (See figure 3.) Suppose we assume that variations in the atmospheric pressure field during this interval indeed are the result of scattered infrasonic waves whose speed range is bracketed by the values c_ℓ and c_u. If the field is stationary in time and homogeneous in a plane parallel to the

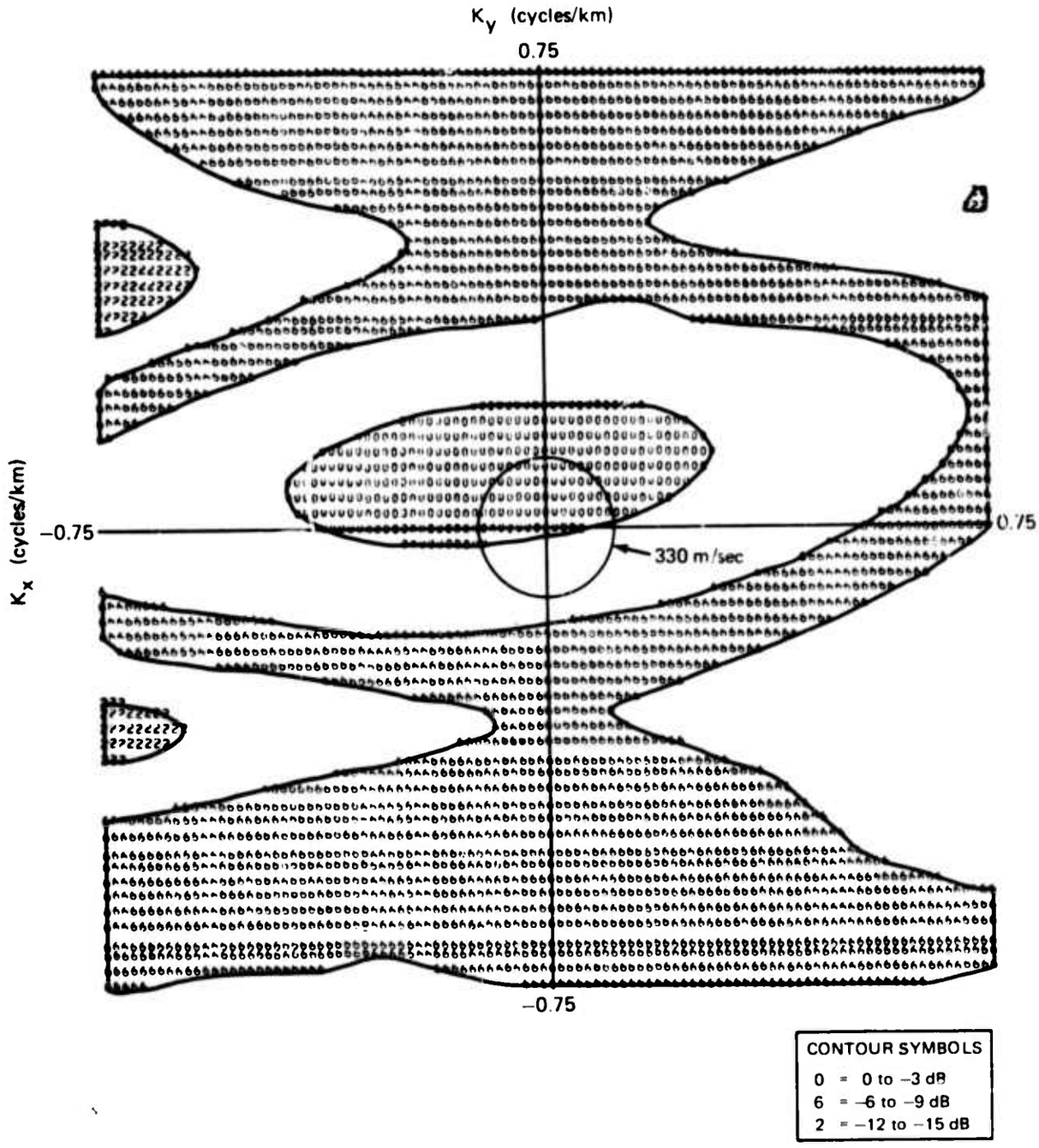

Figure 3. Distribution of pressure on the wave number plane at a period of 26.95 seconds. Results indicate a source of infrasonic atmospheric pressure variations from the northwest, McKinney, Texas.

G 7573

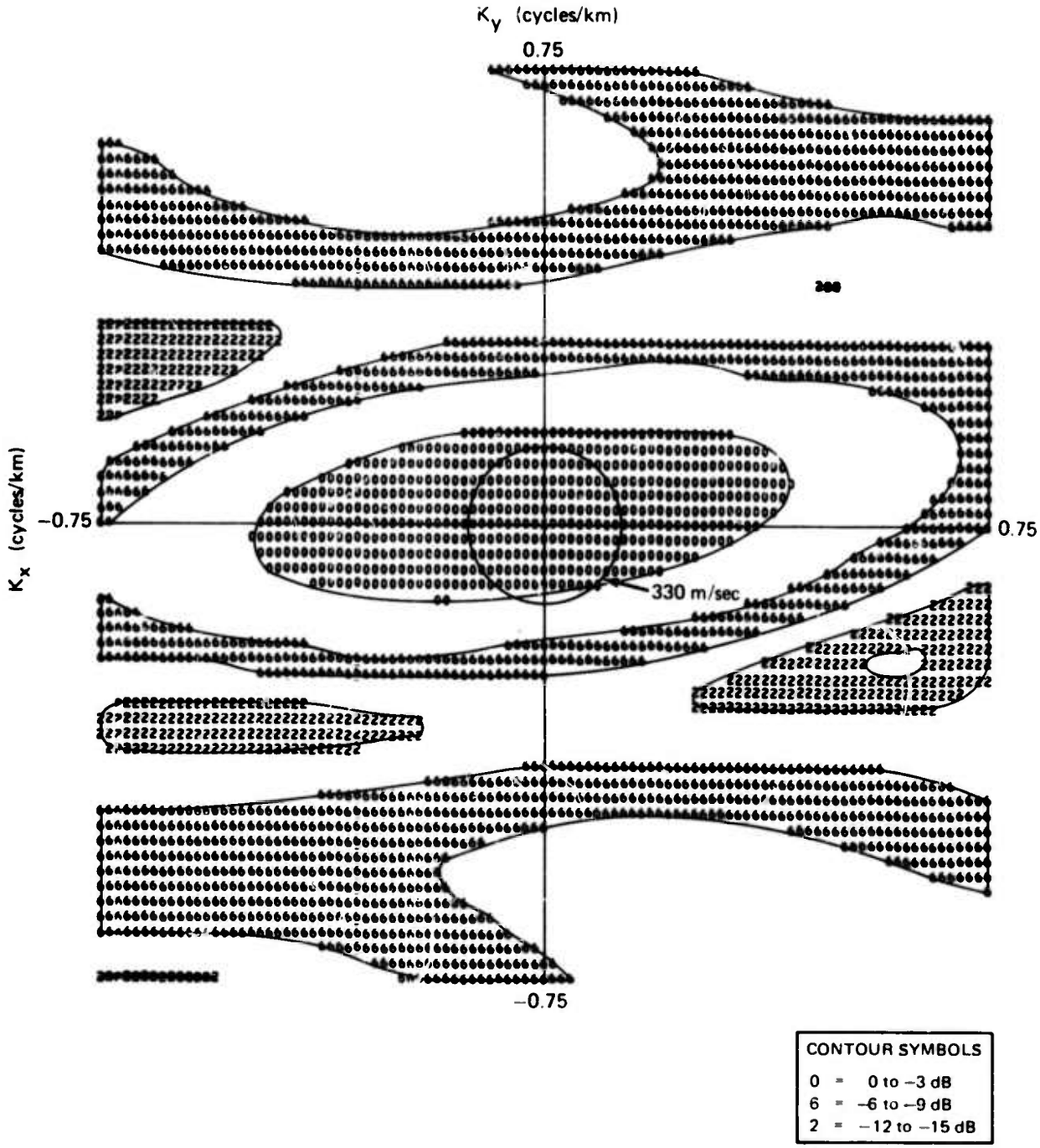

Figure 4. Distribution of pressure on the wave number plane at a period of 23.27 seconds. Results indicate a source of pressure variations at 960 m/sec from the west, McKinney, Texas.

G 8356

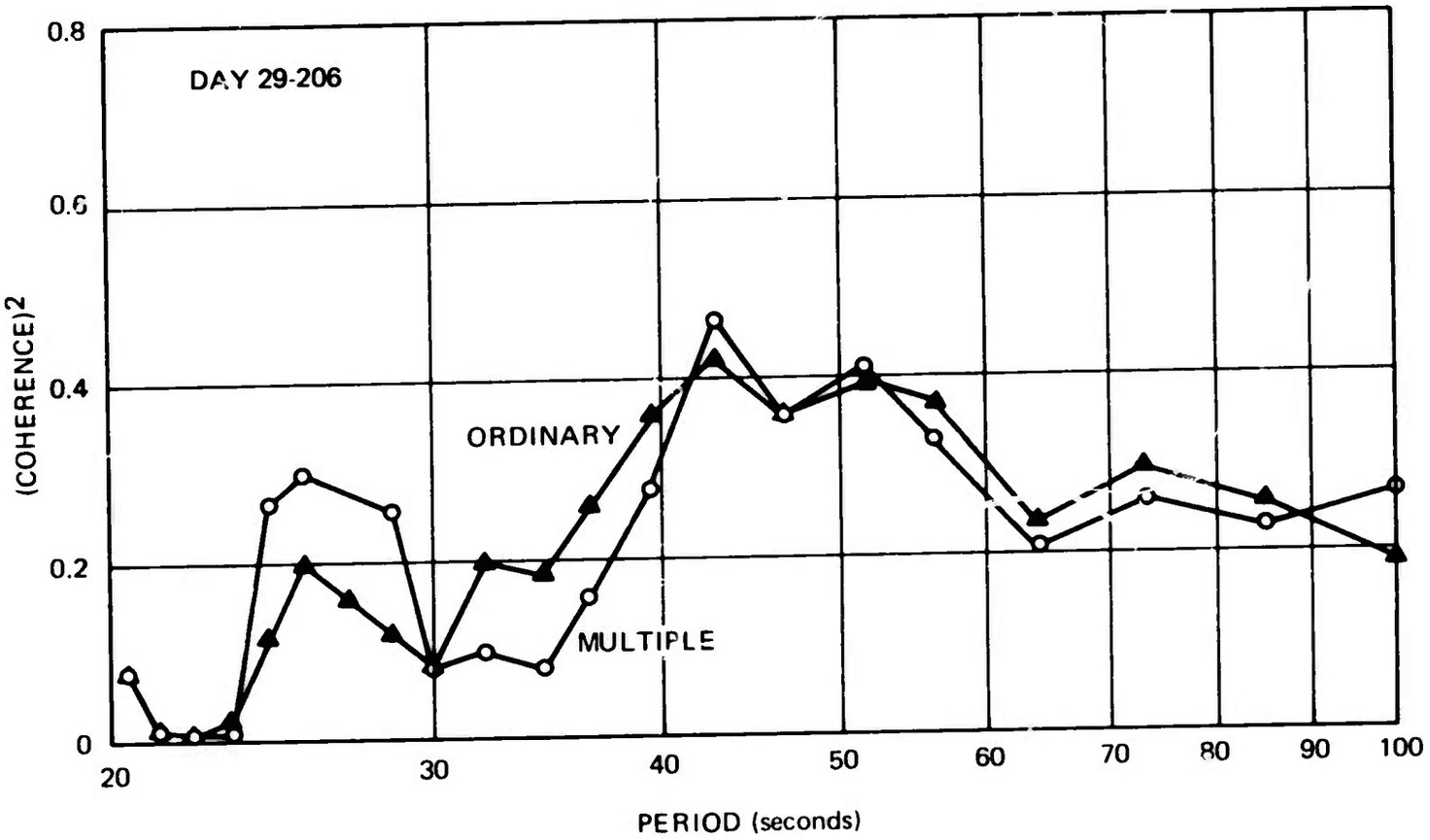

Figure 5. Estimated squares of the ordinary and multiple coherence between the outputs of a vertical seismograph and selected elements of the microbarograph array during a calm interval on 29 January 1974, McKinney, Texas. Estimated squares of the ordinary coherence which fall below the dashed line are not significantly different from zero at the 90 percent confidence level.

G 7572

earth's surface and the power spectra of the waves are independent of their speeds, then for the case of a vertical seismograph and a microbarograph located at the surface of a homogeneous and isotropic half space, the square of the ordinary coherence is given by

$$\gamma^2_{MZ}(\omega) = \left\{ 2 \left(\frac{\frac{c_u}{c_\ell} - 1}{\frac{c_u}{c_\ell} + 1} \right) \cdot \frac{1}{\log_e \left(\frac{c_u}{c_\ell} \right)} \right\} \phi(\omega) \qquad (19)$$

(Sorrells and Goforth, 1973, eq. 61)

where $\phi(\omega)$ is the percentage of seismic noise power caused by atmospheric pressure variations. The term in brackets is the ratio of predictable pressure related noise power to total pressure related noise power.

This ratio decreases monotonically as the c_u increases with respect to c_ℓ (i.e., as the speed range of the scattered waves expands). Now one would expect the speed range of scattered infrasonic waves to be no greater than about 300-600 meters/second $\left(\frac{c_u}{c_\ell} \leq 2 \right)$.

For a speed range of this order the ratio of predictable to total power is greater than 0.9. Thus, from equation (19) the square of the ordinary coherence will underestimate the percentage of pressure related noise power by 10 percent or less. Since the square of the multiple coherence is always greater than or equal to the square of the ordinary coherence but less than or equal to the percentage of pressure related noise power it follows that in the case of scattered infrasonic waves the ordinary and multiple coherences should be approximately the same. It is therefore our belief that the results in figure 5 together with data from the frequency-wave number estimates indicate that infrasonic waves are the principal source of the atmospheric pressure variations and pressure related earth noise observed during this interval.

It should be noted that relatively very minor amounts of wind-generated noise are sufficient to obscure the infrasound-associated relationship between the seismographs and microbarographs. But in the seismic background spectra the percentage of pressure-related noise caused by wind is less than 10 percent of the total of such noise, except when the power of the wind pressures exceeds that of the infrasonic component by fully a factor of 20 or more in the microbarograph spectra. This illustrates the point that though the contribution of infrasonic waves to the pressure spectra may be relatively small, it may still account for virtually all of the pressure related earth noise found in the vertical seismic noise spectra.

When examining the numerous spectra of the noise obtained from the seismometers at Pinedale, where the seismographs are unaffected by the wind, it is clear that at times there is considerable structure in the noise in the

notch observed at 20-40 seconds of period. Small but statistically significant peaks are present; the reasons for believing they consist of seismic energy are:

a. They appear on both horizontals and verticals at about the same power in the same fashion as the microseismic peaks at 18- and 6-second periods. If they were associated with environmental noise one would expect them to be considerably larger on the horizontals, which, because of their tilt sensitivity, almost invariably are more susceptible to environmental noise.

b. Associated with the peak in the spectra there is usually an increase in coherence between instruments of the same orientation operating at different depths.

c. They do not appear to be related to the atmosphere as there is never a corresponding peak in the power spectra of the microbarograph or any increase in the coherence between any seismometer and the microbarograph. Furthermore, when peaks in quiet day spectra were found at McKinney, the frequency-wave number spectra did not show any long-wavelength atmospheric phenomena at the corresponding periods.

It will require an array of high-quality, buried, long-period seismographs such as is presently being constructed in Iran to verify the conclusion that there is appreciable seismic energy at periods of 20 to 60 seconds.

5. PREDICTION

The experiments in predicting long-period noise were carried out at McKinney, Texas, because the required microbarographs were available at this site. Unfortunately, even during windless intervals, only the vertical long-period seismographs could be operated at magnifications comparable to those attainable at some depth below the surface. The horizontal seismographs are noisy even during windless periods and the prediction filtering techniques for the horizontals were far less effective than for the vertical seismographs.

5.1 WINDY PERIODS: VERTICAL SEISMOGRAPHS

Amplitudes of wind-induced pressure variations can easily be 1 to 2 orders of magnitude greater than long wavelength infrasonic or other atmospheric phenomena detected during windless periods. Therefore, during intervals of moderately high wind speeds (> 4 m/sec), the pressure-related noise will be dominated by quasi-static deformations in response to the wind-generated pressure variations. Because of the short wavelengths associated with wind-induced turbulence, correlation is found only between the outputs of the seismographs and the co-located microbarograph. It is therefore unnecessary to include the outputs of the other microbarographs in the processing; the experimental problem thus simplifies to the estimation of single-channel optimum filters.

In the following, note that none of the spectra of this section are corrected for system response.

Figure 6 shows the results of one of the experiments; shown are the spectra of the vertical earth noise as recorded by the seismograph and the noise after the predictable portion of the noise had been subtracted. The wind was blowing approximately 8 m/sec during this time. The required auto- and cross-correlation were computed from a 2-hour sample and the calculated filter applied to the same time interval. The filter used was 58 points (232 seconds) long and had no delay built in; several filters with different delays were tried but no improvement could be obtained by using a non-realizable filter. Examination of figure 6 shows clearly that a large percentage of the earth noise is caused by wind-induced pressure variations because this noise was effectively predicted by an optimum filter based on the microbarograph output. In order to show the effectiveness of the process, the earth noise on a windless day (about a week before) is also included. It has been found that in the absence of wind related earth noise, the spectrum of the vertical component of the noise remains approximately stationary (within 6 dB) for intervals at least on the order of a month. As expected, at periods of 20 seconds and less the filter is ineffective because the microseisms predominate in the earth noise. Examination of the mean square error shows that 55 percent of the total power was predictable with this filter. The total power includes the microseisms; in the band from 20- to 100-second periods, the percentage of predicted energy is considerably greater.

Figure 7 shows a plot of average wind velocity versus the percentage of total energy that can be predicted with a single-channel filter. The filters were all computed from 1-hour sample times when the wind was fairly constant. While there is considerable scatter in the data points there is, as expected, a distinct increase of prediction capability with increasing level of wind and therefore, atmospherically-generated earth noise. The scatter of the points is at least partly caused by variations of the power level of the microseisms. Despite the variability shown in figure 7 the stability of the computed filters is good, as will be discussed later in this section.

The single channel optimum filters discussed in the paragraphs above were estimated from data recorded during a finite interval of time. They were then used with considerable success to reduce seismic noise levels over the same interval. However, in practice, it is certainly desirable and sometimes necessary to apply the filters computed for one interval to the data recorded during other intervals as well. Information regarding the temporal stability of the filter estimates is, therefore, of considerable practical importance. In order to obtain such information we computed filters from seventy-six 1-hour samples spanning a 2-week interval. Typical estimates of the modulus and phase of the filter transfer functions are shown in figures 8 and 9. These results were obtained from data recorded during six of the intervals when the mean wind velocity was 6-7 m/sec from the south. The dashed curves bracket the 90 percent confidence interval for sample 78-0500. These results imply that the observed scatter can be attributed to normal statistical variability. It is important to note that the data from which these filters were estimated were taken only during intervals when the mean wind speed and direction were approximately the same. Theoretical considerations (Sorrells, 1971), lead us to expect systematic changes in the filters

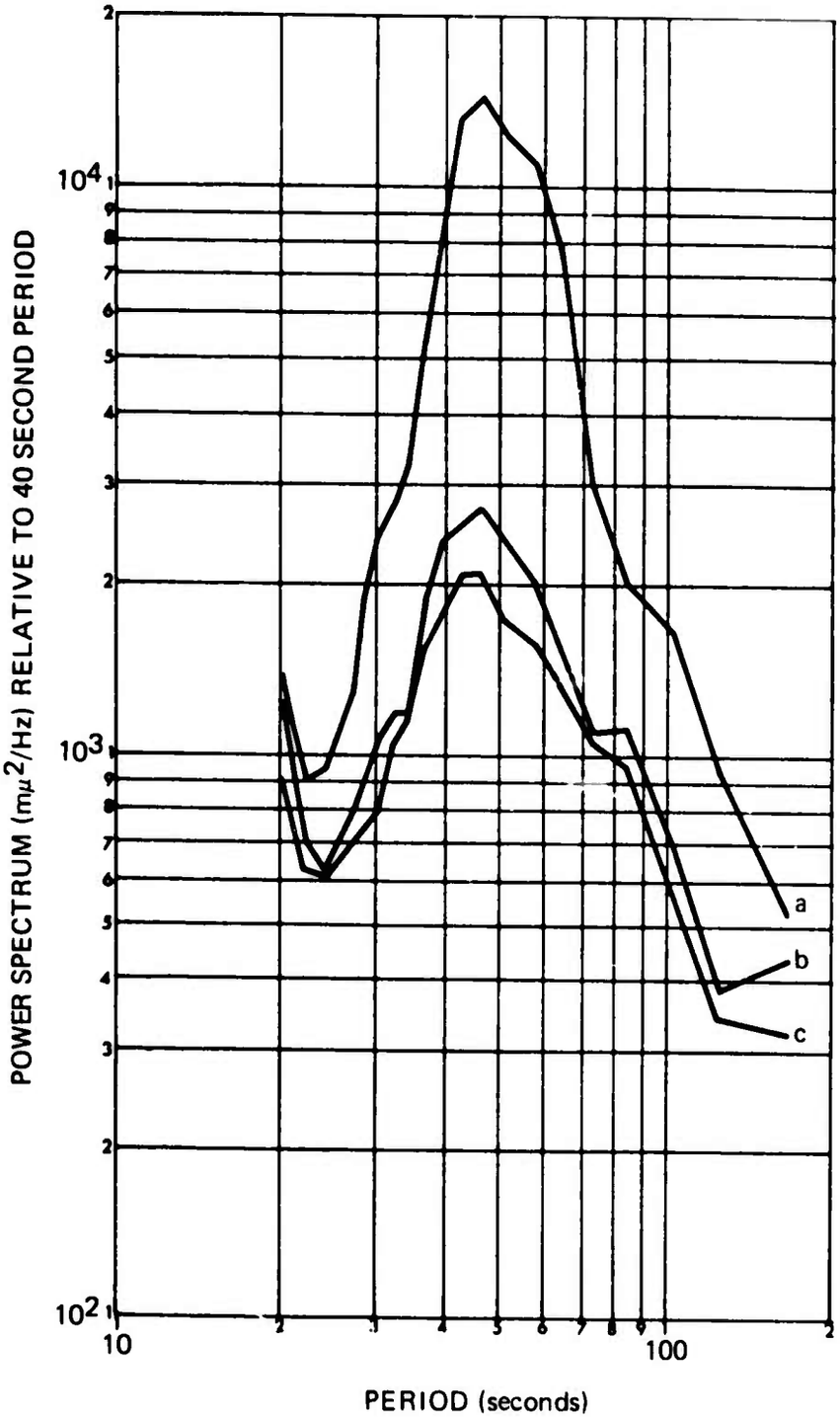

Figure 6. Power spectra of the noise recorded by a vertical seismograph (a) original recording, (b) after signal channel optimum filter, (c) quiet day spectrum. Wind velocity 8 m/sec, McKinney, Texas.

G 7533

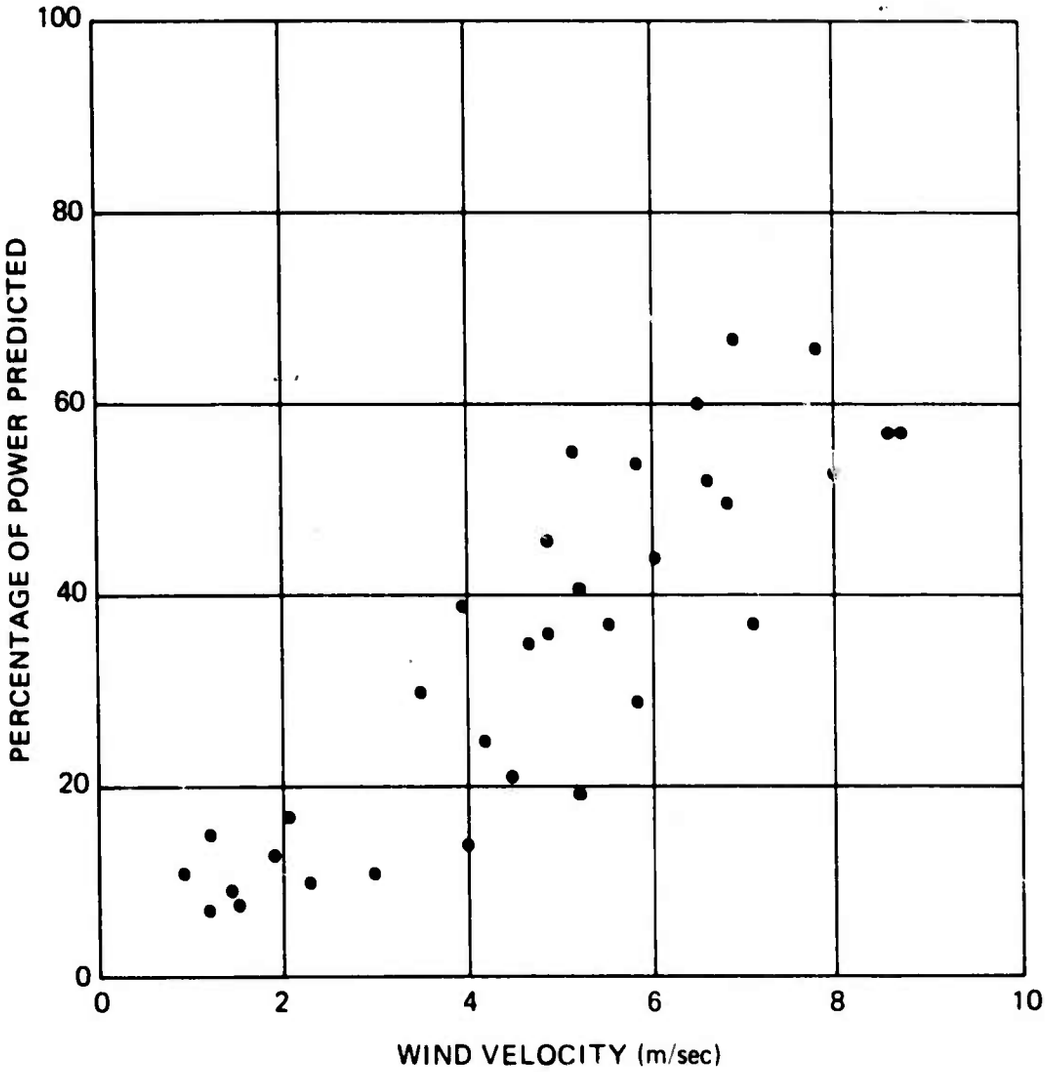

Figure 7. Average wind velocity versus the percentage of total power predicted by a single-channel filter, McKinney, Texas.

G 7534

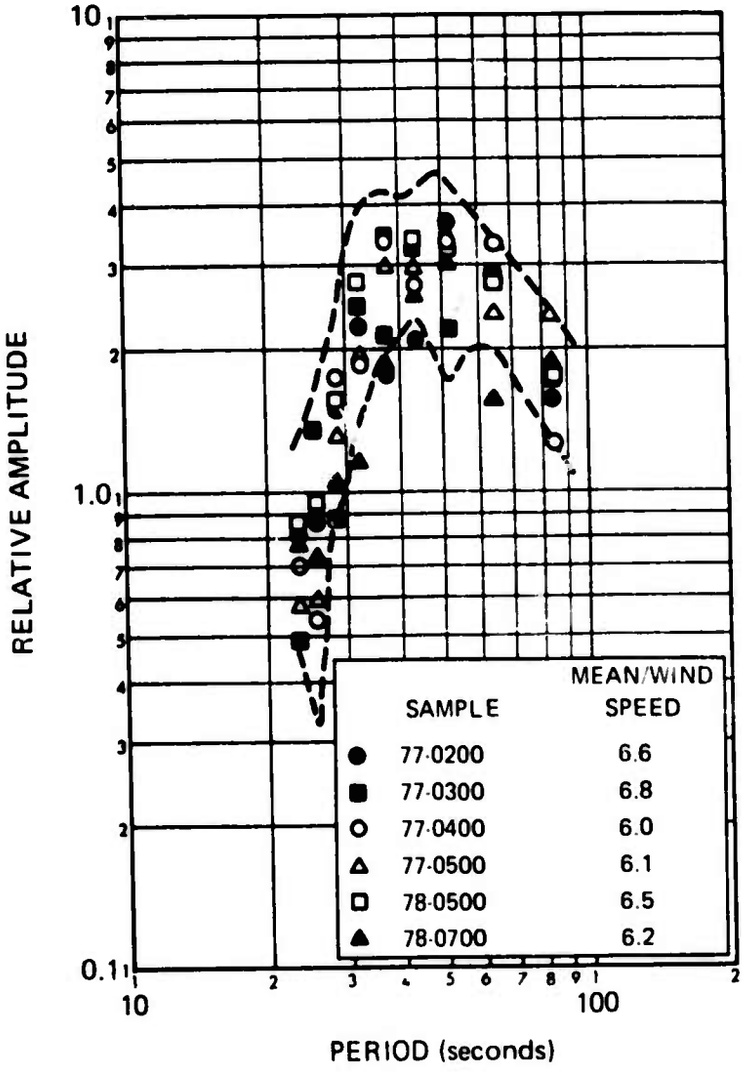

Figure 8. Moduli of the transfer functions of the optimum filters used to reduce noise on the vertical seismograms, McKinney, Texas.

G 7536

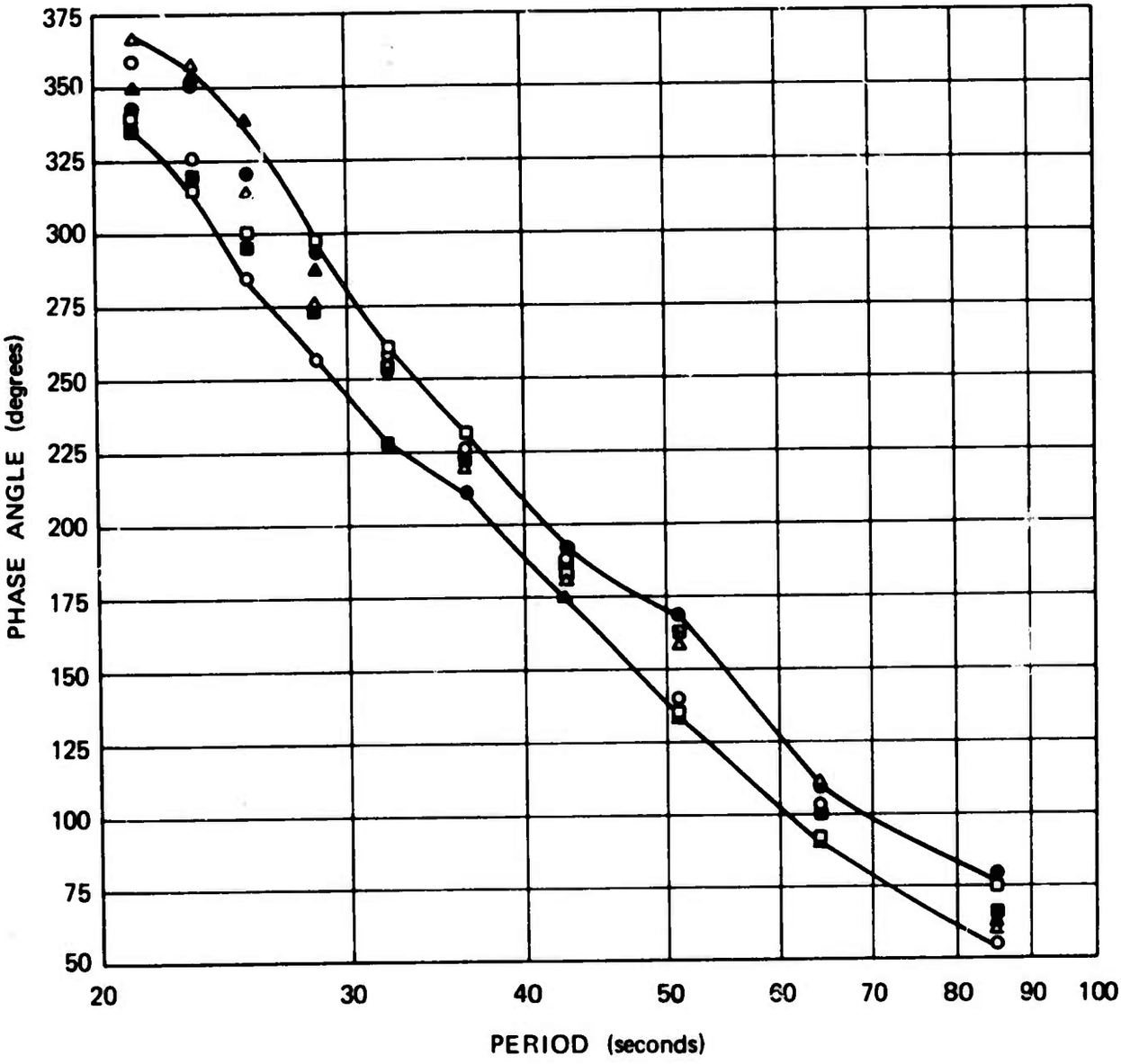

Figure 9. Phase of the optimum filters used to reduce noise on the vertical seismograms, McKinney, Texas.

G 7537

as the mean wind speed and direction changes. For example, in the case of the homogeneous and isotropic half space, the modulus of the vertical filter should increase in proportion to the mean wind speed while the phase remains constant. On the other hand, the modulus of the horizontal filter should be independent of the wind speed but should vary as the cosine of the angle between the sensitive axis of the seismograph and wind direction. In addition the phase should remain constant as long as the wind direction remains within ±90 degrees of the positive direction of the sensitive axis. If it exceeds these limits, the phase of the filters should shift by 180 degrees.

In order to detect the anticipated changes in the vertical filter, we have computed the average modulus and phase for the 4-6, 6-8, and 8-10 m/sec wind speed ranges. These are shown in figures 10 and 11. As expected the modulus increases as the wind speed increases while the phase remains constant. Our data base is not currently adequate to demonstrate the cosine dependence of the modulus of the horizontal filter, as the wind was either out of the north or the south during the 2-week interval selected for detailed study. However, the preliminary results suggest that the modulus of the horizontal filter is independent of the wind speed as implied by the theory.

On the basis of these results, we may infer that the optimum filters will remain stable as long as the mean wind speed and direction remain approximately stationary. It has been our experience that, apart from the situation during frontal passages, these quantities tend to vary slowly and smoothly with time. In the north Texas area, for example, the wind direction may remain roughly constant for periods of time on the order of days, while the mean wind speed undergoes a smooth diurnal variation. It is also important to observe that the filters for the vertical seismograph vary in a predictable fashion with respect to the mean wind speed and direction. These results suggested that time varying filters whose properties change in response to changes in the mean wind could be used to effectively remove wind-generated noise. However, a few preliminary tests of this approach, using adaptive filters based on the Widrow algorith (Widrow, 1968), were not successful, primarily because of instability in the process. Further investigations are required to show whether such an adaptive filtering technique based directly on mean wind speed and direction will prove superior to the one used above.

To present examples of the improvements obtained on seismograms, visually, which is the way most seismic traces are analyzed, we show (figure 12) a couple of representative cases, one for noise only on a horizontal and one for a vertical with a signal. In each of the two cases, the top trace is the original recording. The middle trace shows the output of a single-channel prediction filter, and the bottom trace is the result of subtracting the predicted time series from the original recording. In both cases, the wind was blowing 8-10 m/sec, and the auto- and cross-correlations for the filter design were estimated from 1 hour of data. The noticeable phase shift between the original and predicted traces is a function of the particular data. In other parts of the same records these slight phase shifts are different. Figure 12b shows the results of applying the technique to the surface wave group associated with an earthquake with an m_b of 3.6 that occurred south of Panama approximately 31 degrees south of our site. Notice how the onset of the surface waves on the observed vertical seismograph has been obscured by the almost simultaneous arrival of a wind-generated noise pulse shown on the

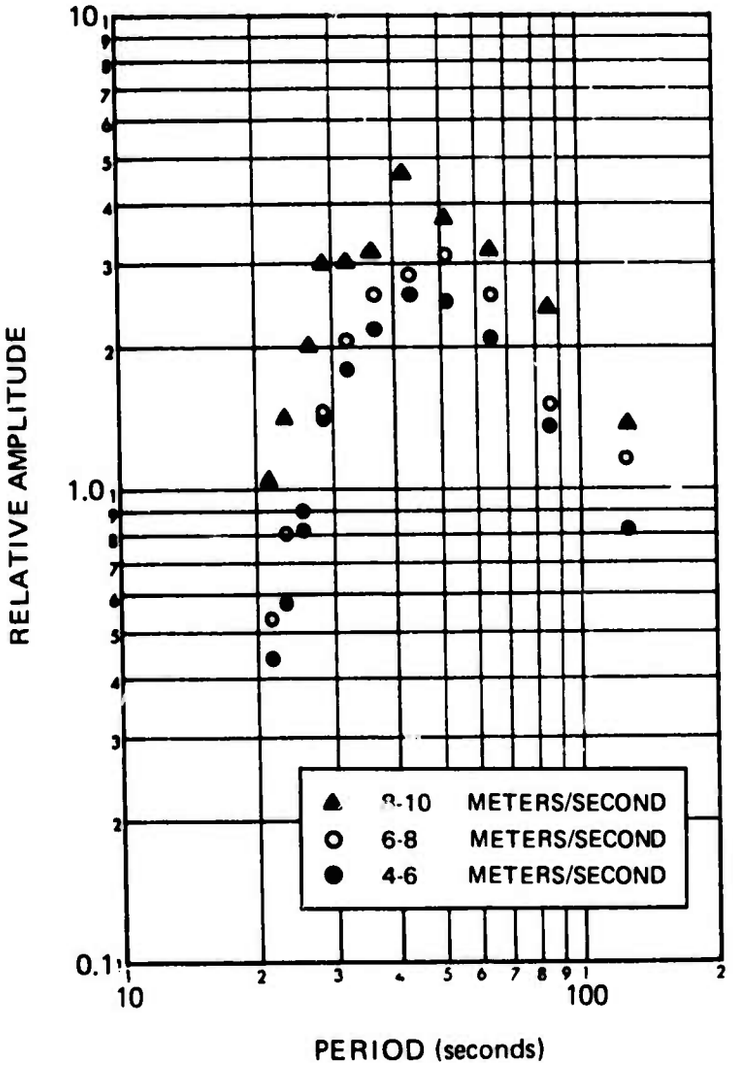

Figure 10. A comparison of the average moduli of the vertical optimum filters for various mean wind speeds, McKinney, Texas.

G 7538

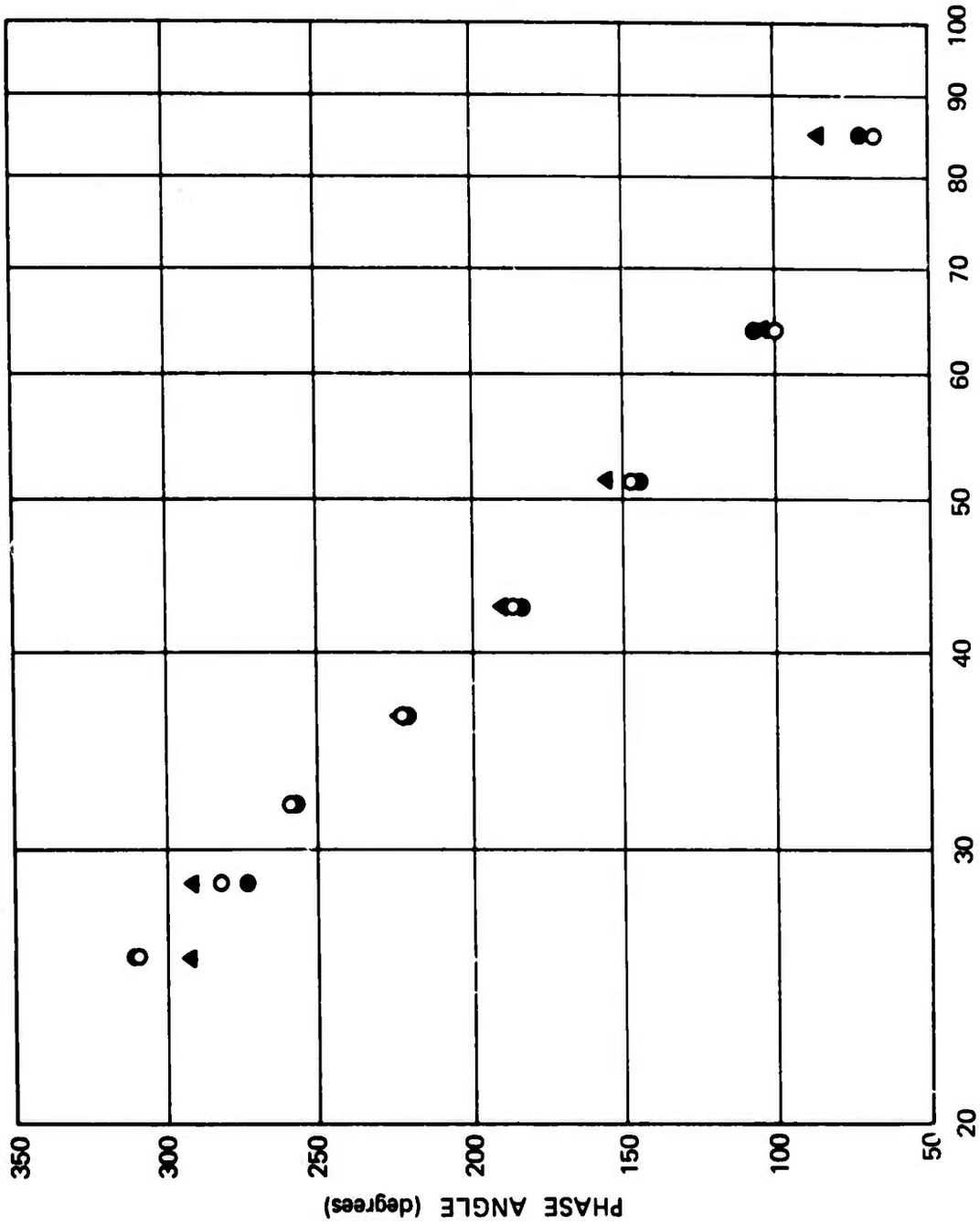

G 7539

Figure 11. A comparison of the vertical optimum filters for various wind speed ranges, McKinney, Texas.

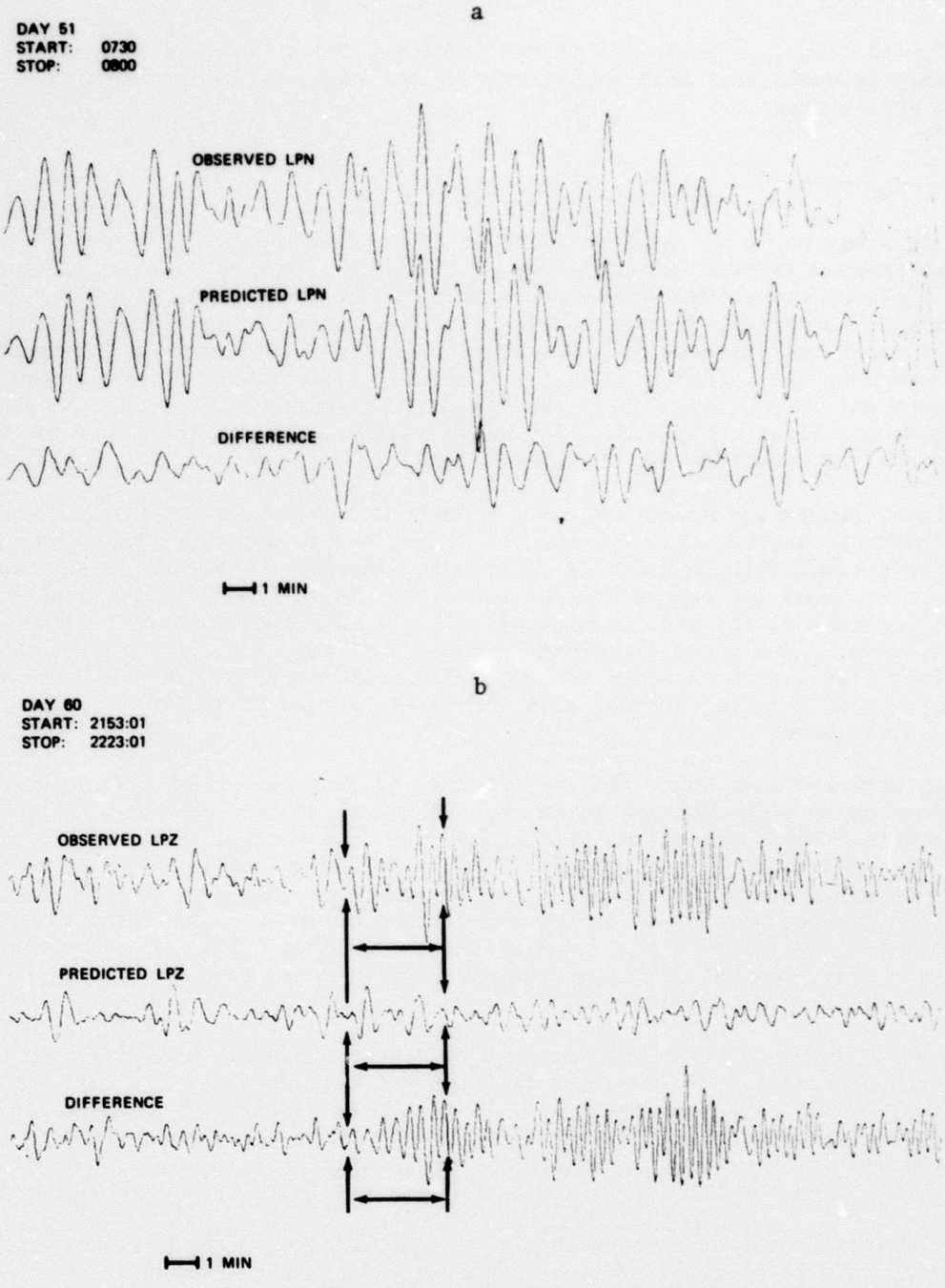

Figure 12. Observed and optimum filtered seismograms (a) noise recorded by horizontal seismograph (LPN), (b) signal recorded by vertical seismograph (LPZ).

G 7540

predicted trace. Subtraction of the predicted trace from the observed seismogram works very well in cleaning up the early cycle or two of the surface wave group.

5.2 CALM PERIODS: VERTICAL SEISMOGRAPHS

During windy periods, single-channel optimum filtering of the vault microbarogram is effective in reducing its noise. During windless periods (<1.0 m/sec) the nature of the pressure field is far more complex. As discussed in section 4, frequency-wave number analysis of the microbarograph array shows the presence of multiple sources and a wide range of velocities. The array is not sufficiently large to clearly differentiate between these sources and velocities, for it was designed to study the 6-second microbaroms. At present, it is not possible for us to make definite statements about the nature of the pressure field on quiet days.

Because computation of multichannel filters is time consuming, the multiple coherence in a given case was usually calculated to determine beforehand if the optimum filters would be effective. The results varied considerably. Figure 13 shows two representative examples. As mentioned in the section on data processing, the bias problem of multiple coherence is severe; shown on the figure is the expected zero coherence level computed according to the maximum likelihood technique (White, 1973). The samples were taken 5 days apart and only six microbarographs were used because of instrumentation problems with number 2.

It is apparent from these results (figure 13) that there would be a large difference in effectiveness of the multichannel filters for these two intervals. For 1 day the multiple coherence is essentially negligible except for one peak at 39 seconds, and multichannel filters would not predict the seismograph noise. For the other day the multiple coherence is significantly above the expected zero level for the periods between 40 and 128 seconds; thus the filters would effectively reduce the noise level. This second curve closely resembles the multiple coherences of the data used to compute the optimum filters described below.

Figure 14 shows an example of optimum filtering during a quiet day when the coherence measurements indicated clearly that multichannel filtering would be effective, while the coherence between the seismograph and the vault microbarograph showed that a single-channel filter reduced the power level only marginally. The results are quite clear; however, the improvement is not as great on this quiet day as it is for intervals with wind-generated noise.

The sources in the atmosphere that were contributing to the pressure-induced noise on the seismograph at the time these filters were computed were probably low level infrasonic waves. The frequency-wave number spectrum shows that the energy between 50-60 second periods is at least partially the result of acoustic waves from the northwest. However, the large difference in predictability from single- to four-channel filters clearly indicates that the acoustic waves are not the only source of pressure variations.

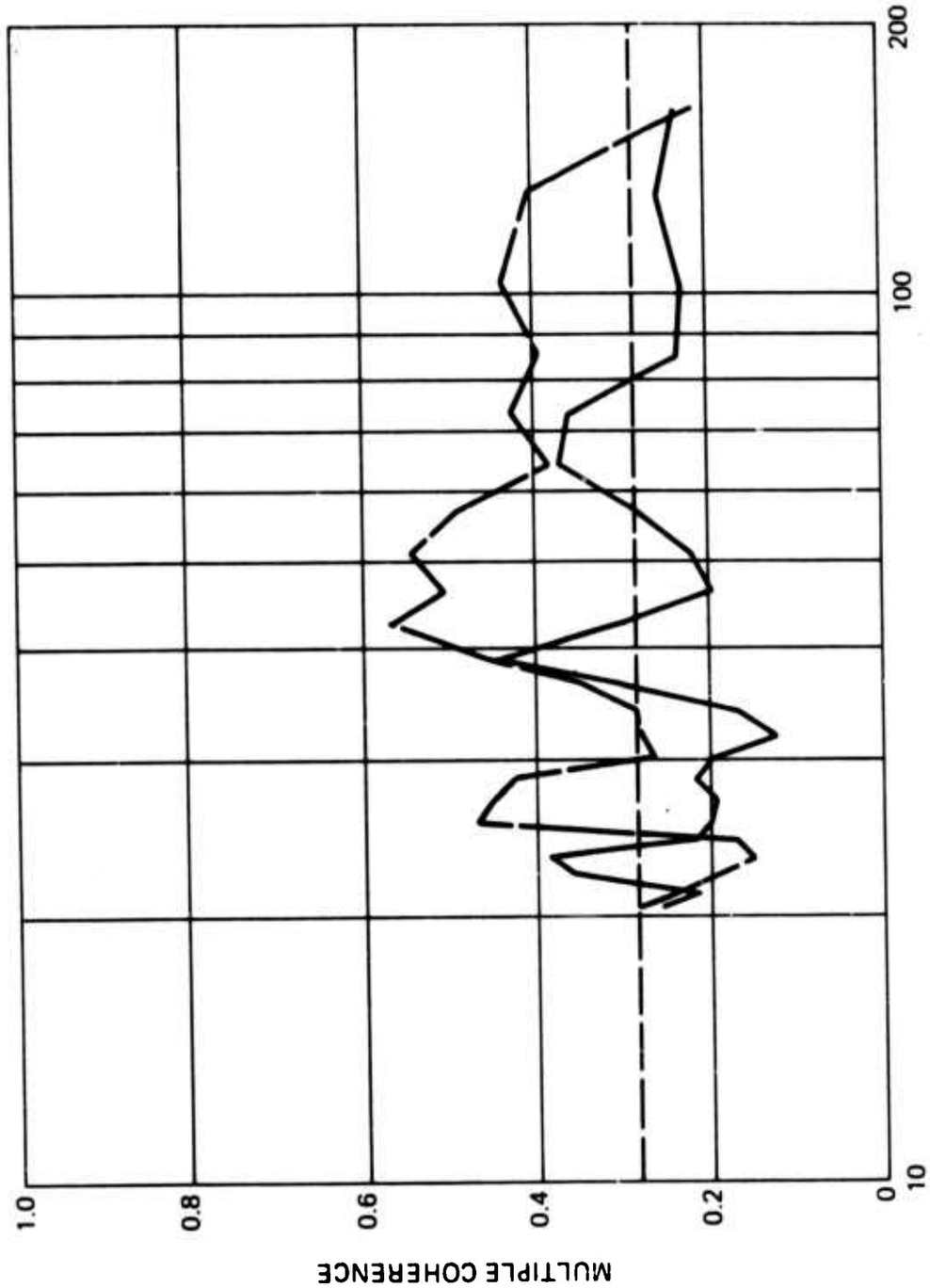

G 7541

Figure 13. Two examples of multiple coherences obtained on windless days. Vertical seismograph at McKinney, Texas.

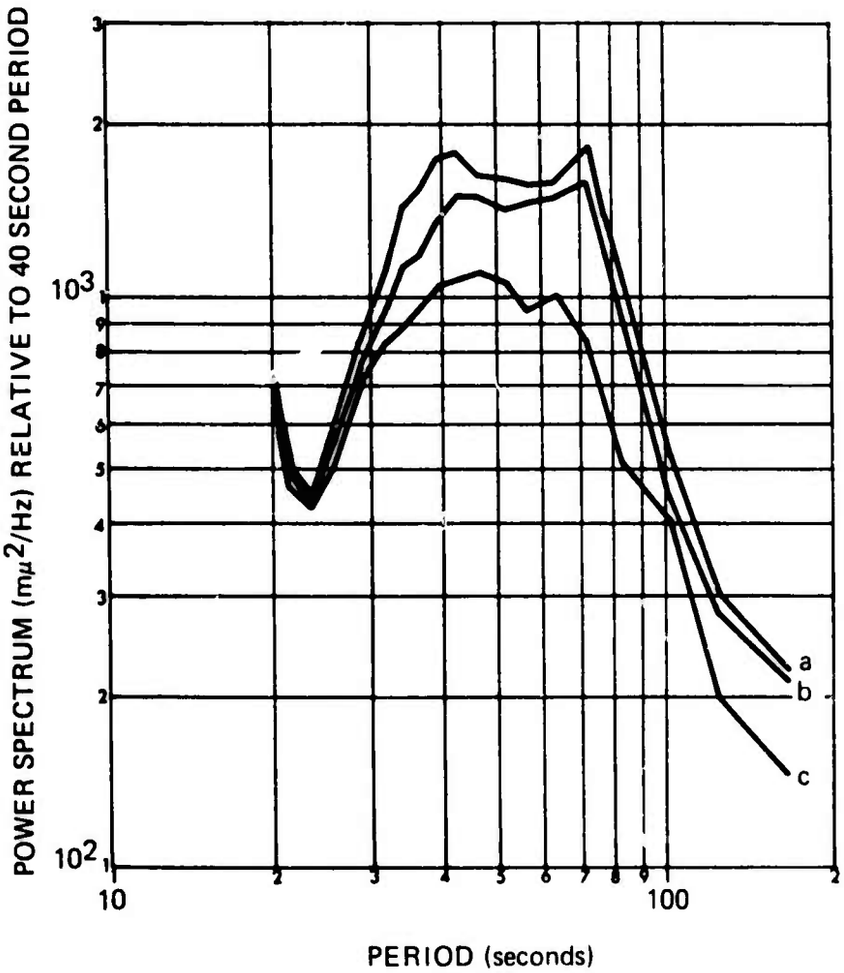

Figure 14. Power spectra of the noise on a vertical seismograph during a windless day. (a) original recording, (b) single-channel filter, (c) 4-channel optimum filters, McKinney, Texas.

G 7542

Out of the total power recorded by the seismograph, the single-channel filter could only predict 13 percent; the four-channel set of optimum filters predicted 30 percent when 256-second (64-point) filters were used, and could have predicted 20 percent with 80-second (20-point) filters. This is, of course, only one example. Each case shows different results, with short filters sometimes being as effective as the longer ones.

5.3 HORIZONTAL SEISMOGRAPHS

The discussion of prediction filtering up to this point applies to its application to vertical seismographs. As mentioned previously, the horizontal seismographs at McKinney were noisy even during windless periods. A large number of single and multichannel filters were computed, and the results proved extremely variable for both windy and windless time periods. No general conclusions can readily be deduced from these experiments; at times the single-channel filter was as effective as the multichannel filters, while the opposite effect was almost as common. Furthermore there were numerous times when no appreciable improvement was obtained from any of the filters. At no time was the noise level of the horizontals reduced to the noise level obtained on a horizontal seismograph located at depth. Figures 15 and 16 show ordinary and multiple coherences between the microbarographs and the north horizontal seismograph for the small (100 m), 5-element microbarograph array located around the vault at McKinney, Texas. These two examples are from windy periods (approximately 6 m/sec) when the coherences obtained were high and the optimum filters were quite effective. In both cases, the multiple coherence and the highest ordinary coherence of the 5 microbarographs is plotted. In one case (figure 15) the microbarograph to the south had the highest coherence with the seismograph while in the other case (figure 16) the vault microbarograph had the highest correlation. It should be noted that in both cases there was at least one microbarograph in this small array that showed practically no correlation with the seismograph. This result over a small array is not completely understood, but it is usually (though not always) those microbarographs whose azimuth from the seismograph is transverse to the orientation of the seismograph that show low coherences. This is to be expected because earth tilting in this direction should not affect the seismometer.

Examination of the figures indicates that optimum filtering was quite effective during these time periods. However, in one case while the south, north and vault microbarographs contribute substantially to the predictability, the east and west microbarographs add little. In the other case, the single-channel optimum filter is as effective as the multichannel filters and computation of a multichannel filter would in no way improve the results.

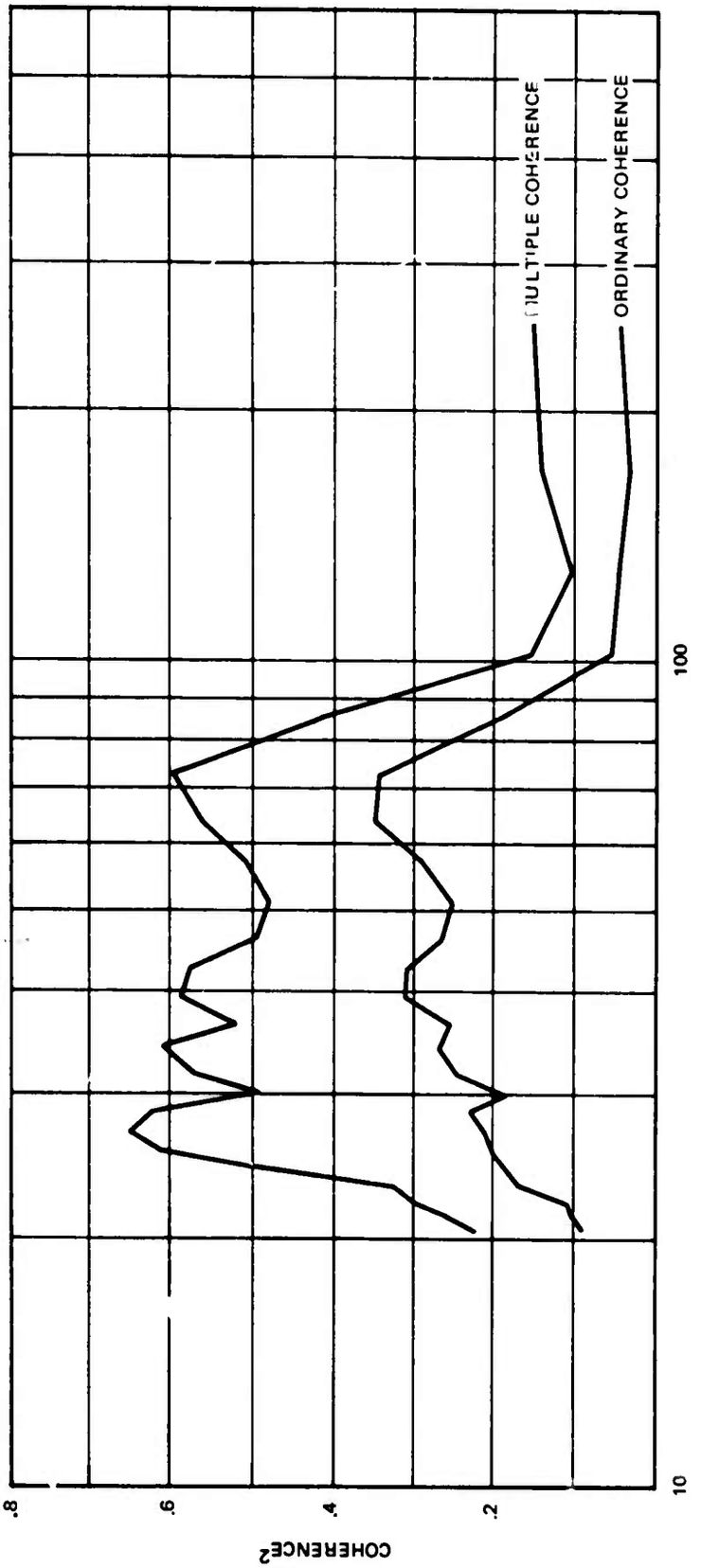

Figure 15. Multiple and ordinary coherence for the north horizontal seismograph and the 100 m, 5-element microbarograph array, McKinney, Texas.

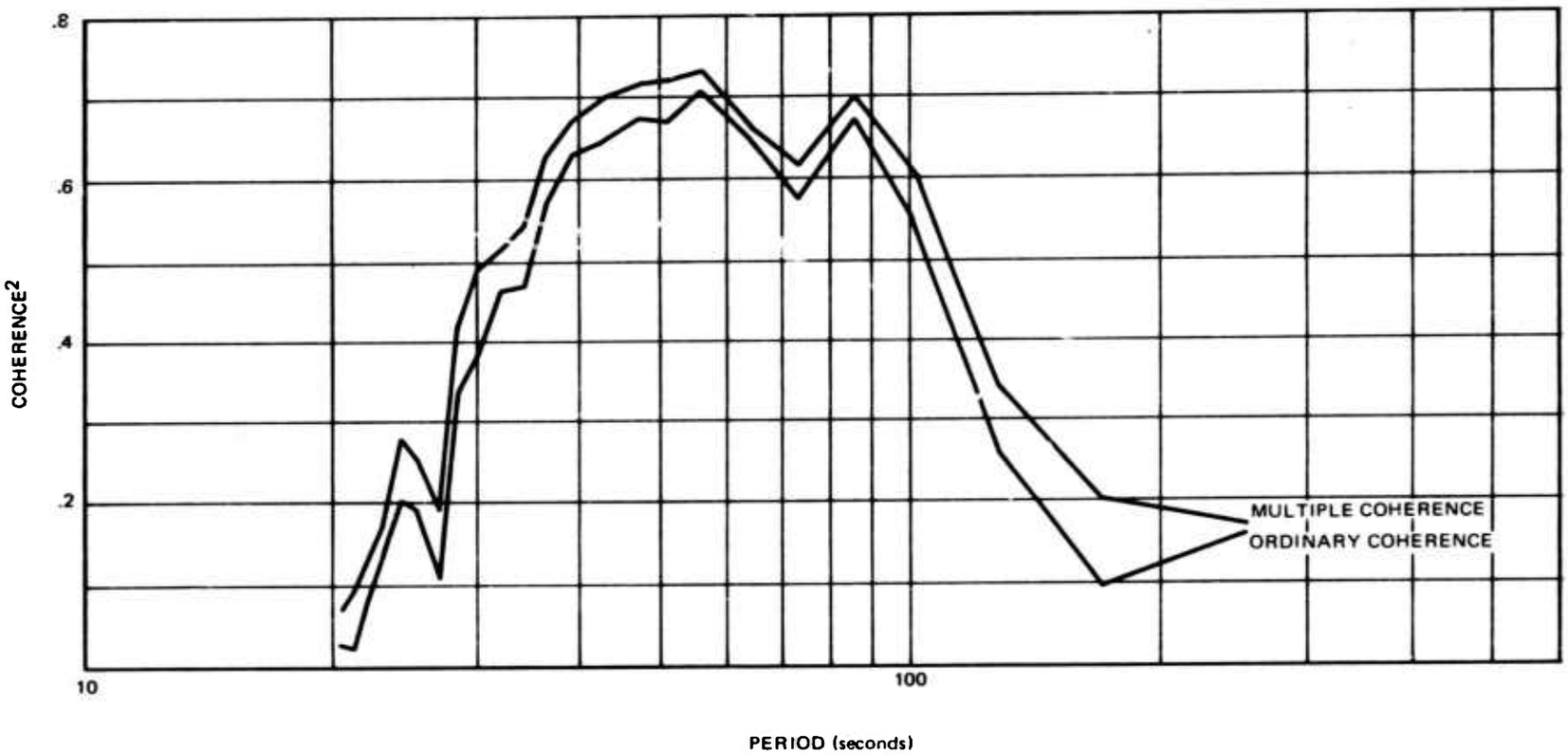

Figure 16. Multiple and ordinary coherence for the north horizontal seismograph and the 100 m, 5-element microbarograph array, McKinney, Texas.

G 8358

6. ATTENUATION OF ATMOSPHERICALLY-GENERATED NOISE WITH GEOLOGY AND DEPTH

During only moderately turbulent atmospheric conditions the magnitude of the wind-generated noise can be as large as 30-60 mμ rms in the vertical direction and 600-1200 mμ rms in the horizontal directions.

Experimental data demonstrate that the effective rigidity of the rocks at or near the surface of the earth is an important factor in determining the magnitude of the transient component. As a simple illustration, consider the following example (see section 2 for theory used). Suppose that long-period seismograph systems are installed at the surface of elastic, isotropic half-spaces whose effective rigidities range from 10^3 to 10^5 bars. This covers a spectrum of rock types varying from poorly consolidated sands and shales to dense limestones and ultrabasic intrusives. Available experimental data indicates that during very calm atmospheric conditions, the noise level in the 20-60 second period range will be roughly the same regardless of rock type. However, when the wind begins to blow, the noise levels will begin to vary. In figure 17 we display the anticipated increase in the 20-60 second noise level produced by a 5 m/sec wind as a function of increasing rigidity. It will be noted that the noise level increases in the horizontal direction are generally much larger than those in the vertical. The reason for this is that pressure generated earth tilts cause apparent horizontal earth motion which is approximately equal to the vertical earth motion multipled by the factor $\frac{gT}{2C}$ where g is the local value of gravity, T is the period of oscillation and C is the convection velocity of the pressure field which is associated with particular period (Sorrells, 1971, Sorrells and Goforth, 1973). In our calculations we have taken C to be equal to the mean wind speed. Thus in our case, in the 20-60 second period range apparent horizontal earth motion will exceed vertical earth motion by a factor which varies from approximately 6 to 19 depending upon the period. It is also important to note that in order to restrict increases in noise levels to 3 dB or less in both the vertical and horizontal directions it is necessary to install the seismographs in rocks with effective rigidities in excess about 3×10^5 bars. Typical rocks with rigidities of this order would be dense limestones or ultrabasic intrusives which possess a low volume percentage of microfractures and cracks. This latter requirement is quite important since results obtained by Nur (1971) demonstrate that the presence of open cracks can cause drastic reductions in the effective rock rigidity.

It has been shown by Sorrells (1971) that earth noise caused by wind-generated pressure decays fairly rapidly with depth. To illustrate this effect we have calculated the noise level increases produced by a 5 m/sec wind at various depths in a homogeneous and isotropic half space. The results are shown in figure 18. For computational pruposes we have assumed an effective rigidity of 10^3 bars, and a Poissons ratio of 0.4. These numbers are representative of very compliant rocks. Observe that in this case placing the seismograph at a depth of 180 meters is approximately equivalent to placing it at the surface of a half space characterised by an effective rigidity of about 3×10^4 bars.

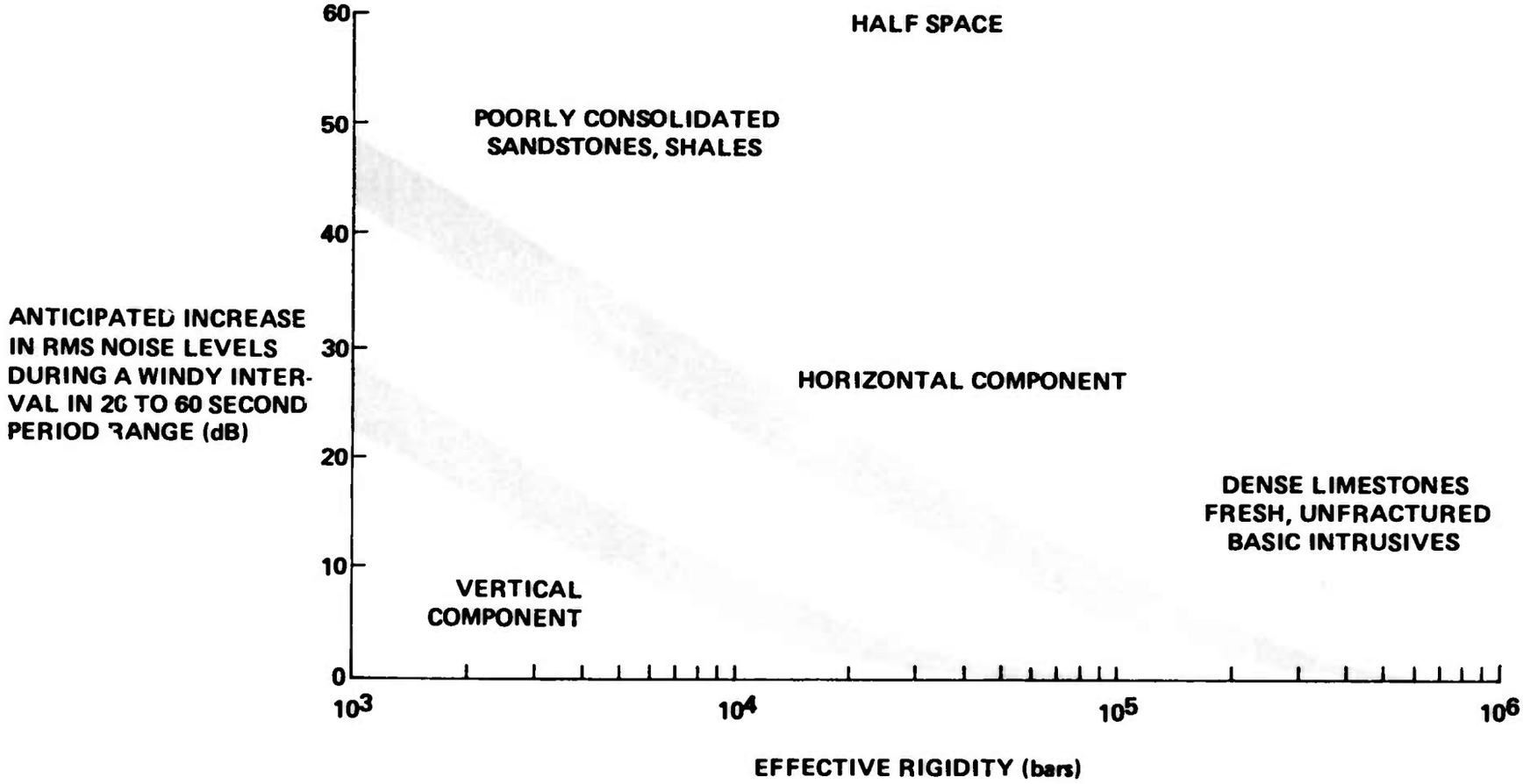

Figure 17. Relative noise level during windy periods vs. rock rigidity (wind - 5 m/sec).

G 8359

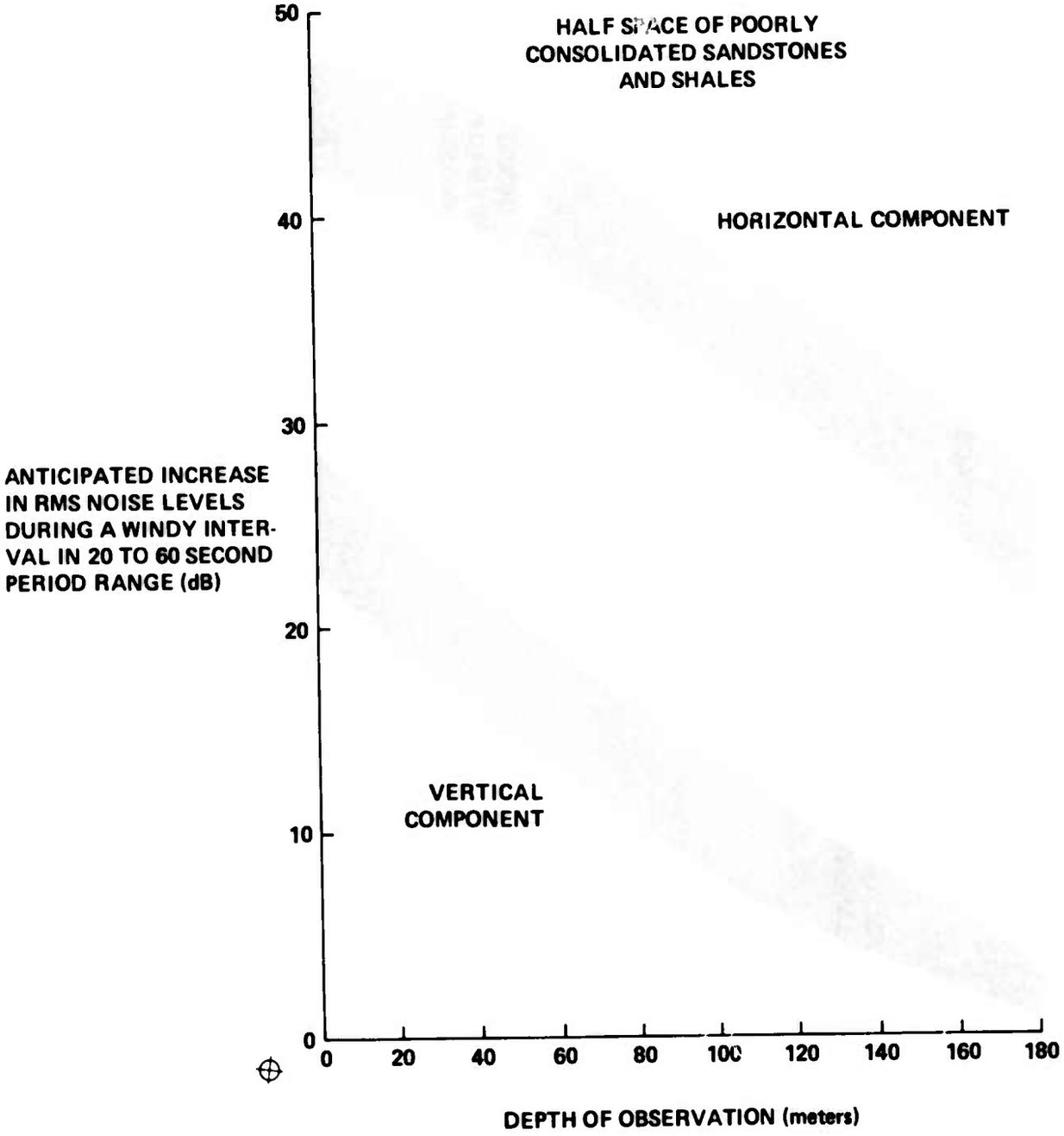

Figure 18. Relative noise level during windy periods as a function of depth (wind - 5 m/sec).

G 8360

In section 2, the theory explaining the attenuation of atmospheric pressure variations was briefly discussed. Experimental evidence to confirm the theory is still limited, although the results show general agreement between them. The main reasons for the lack of confirmation are: (1) seismometers have not been operated at a sufficient number of the shallow depths required to define the amplitude-depth curves; and (2) for horizontal seismographs the environmental effects at the surface make the use of the surface instruments as a reference point extremely difficult.

The main concern in this section is the attenuation of wind-generated noise with depth. The effect of the wind-generated noise decreases rapidly with depth; in most experiments the seismographs were operated at depths far beyond those where the theory predicts wind-generated noise should be recorded. The results of one of these experiments (Douze and Sherwin, 1975) at Pinedale, Wyoming, clearly indicate that the noise levels for both horizontals and vertical seismographs are approximately the same for depths beyond approximately 50 m, where neither wind-generated noise nor surface environmental effects are present. Furthermore, there is no further decrease in the noise level from 50 m down to a depth of 914 m. Figures 19 and 20 show examples of the results obtained at the deep hole site at Pinedale, Wyoming.

Figure 19 shows the noise level of vertical seismographs operating at depths of 46 m and 305 m. The minor differences at the longer periods, with the shallower instrument somewhat noisier, are not significant and probably are caused by differences in system noise levels. Shown in figure 21 is the coherence between the vertical seismographs; the rapid decrease in coherence to the longer periods from the microseismic peak at 20-second period is typical of results obtained. The coherent part must consist of long-wavelength phenomena, elastic waves in the earth or acoustic waves in the atmosphere. However, at periods beyond approximately 50 seconds the noise consists of system noise and environmental effects that do not correlate between seismographs with separations small compared to the wavelengths of atmospheric or seismic noise. Figure 20 shows the noise level of the horizontal seismographs at the depths of 46 and 914 m. Note that the noise level in the notch between 20- and 30-second periods is virtually the same as that recorded by the vertical seismographs at depths beyond 46 m. The more rapid increase in noise level of the deep-hole seismograph towards the longer periods is caused by convection currents (see the appendix). At this depth the seismometer was operating in the water-filled portion of the casing.

At Pinedale, comparisons between the noise levels at the surface instrumentation and the seismographs operating at shallow depth (46 m) did not give clear confirmation of the theory. The expected noise levels were computed using the theory discussed in section 2, the appropriate elastic constants (see introduction), and the experimental pressure variations recorded by the nearby microbarograph.

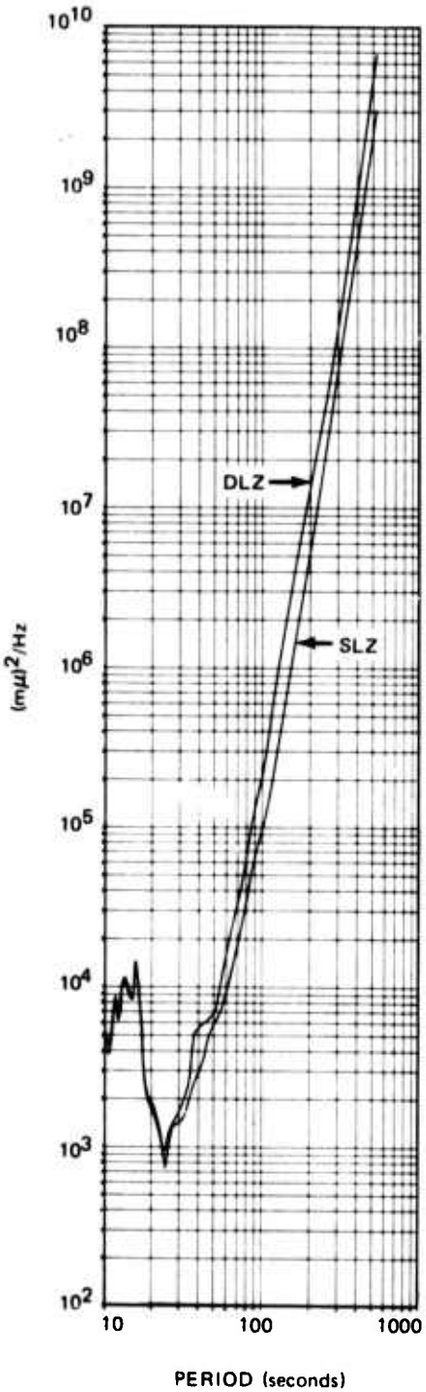

Figure 19. Power spectra of the background noise recorded by vertical seismographs operating at depths of 46 m (SLZ) and 305 m (DLZ). Corrected seismograph response; wind velocity <1.0 m/sec; Pinedale, Wyoming.

G 8361

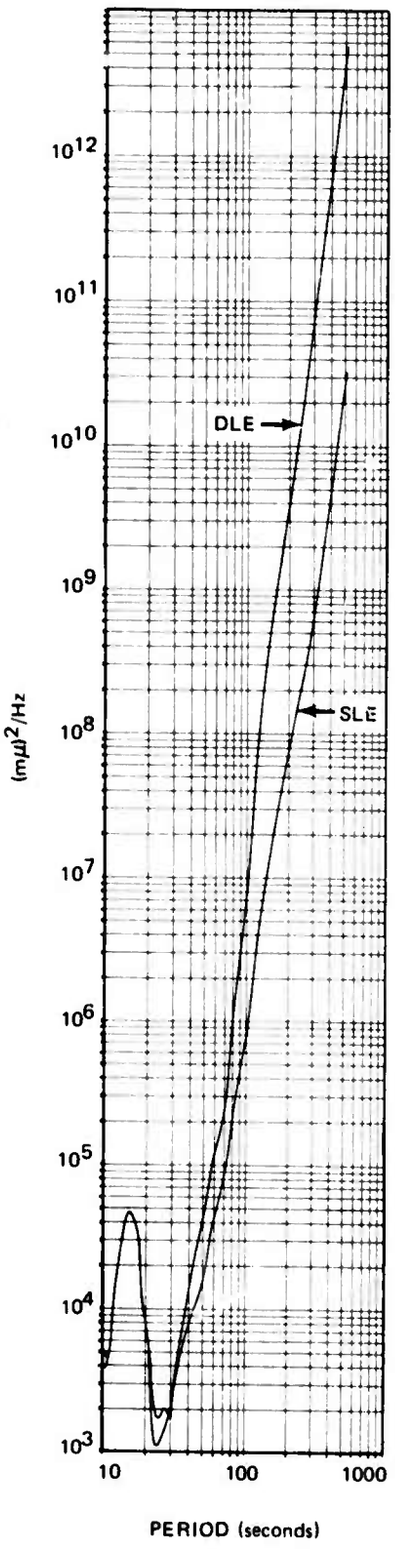

Figure 20. Power spectra of the noise recorded by horizontal (East) seismographs at depth of 46 m (SLE) and 914 m (DLE). Corrected for seismograph response; wind velocity 4.5 m/sec; Pinedale, Wyoming.

G 8362

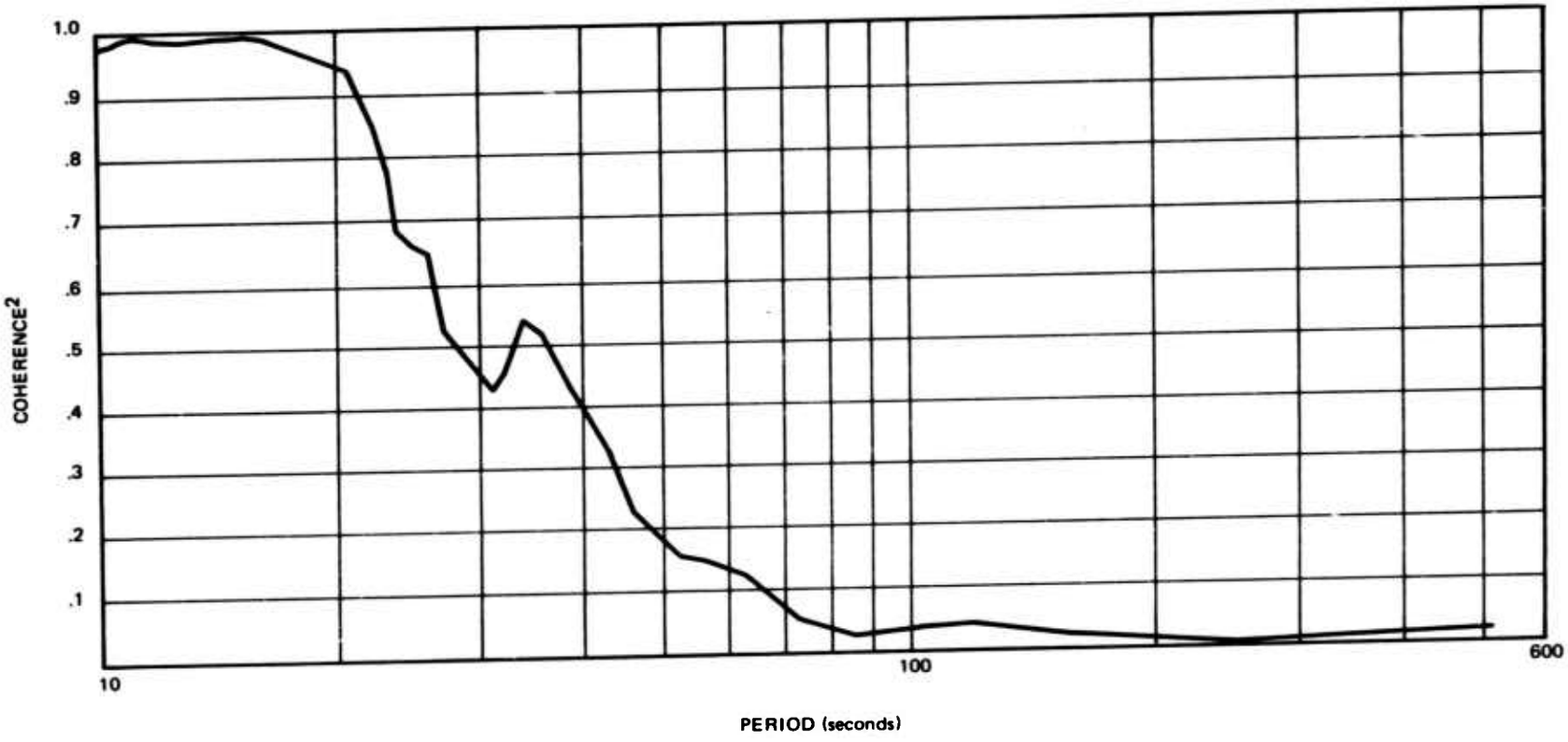

Figure 21. Coherence between vertical seismographs at 46 and 305 m, Pinedale, Wyoming.

G 8363

Figures 22 and 23 show examples of the results obtained experimentally together with the computed theoretical noise levels for the appropriate wind velocities. The theory for vertical seismographs shown in figure 23 clearly indicates that a wind of 5 m/sec should not affect the noise level on either the surface or 46 m seismograph. Beyond the notch there is a difference in the noise levels; the power level of the surface seismograph increases more rapidly than that of the shallow hole seismograph. However, the difference is no larger than that often obtained during windless periods.

For the horizontal seismographs the data are more complex. The surface horizontal noise level increased more than predicted by the theory in the notch (20-30 second period). A suspected leak in the surface valult may be partly responsible for this behavior. At periods beyond 100 seconds the theoretical atmospherically-generated noise level and the actual noise level at 46 m are quite similar. Furthermore, the increase in coherence (see figure 24) between the two seismographs at periods beyond 70 seconds clearly indicates that the two instruments are responding to a common input although the noise level at the surface is still well above that predicted by theory. It is possible that the rigidity at the surface is greatly overestimated because of near surface fractures; this phenomen could account for the discrepancy between theory and the experimental evidence.

At the Grand Saline mine the seismograph at 183 m depth recorded no appreciable amount of wind-generated noise while the surface seismograph noise levels increased by large amounts at this site in sedimentary material (Sorrells et al., 1971). Thus, no direct information on the attenuation of wind-generated noise was obtained. However, during the passage of acoustic waves from a presumed atmospheric explosion the results clearly show that acoustic waves cause deformation at the surface and at 183 m with little attenuation.

In conclusion, evidence collected during these programs cannot conclusively demonstrate the correctness of the theory of wind-induced noise.

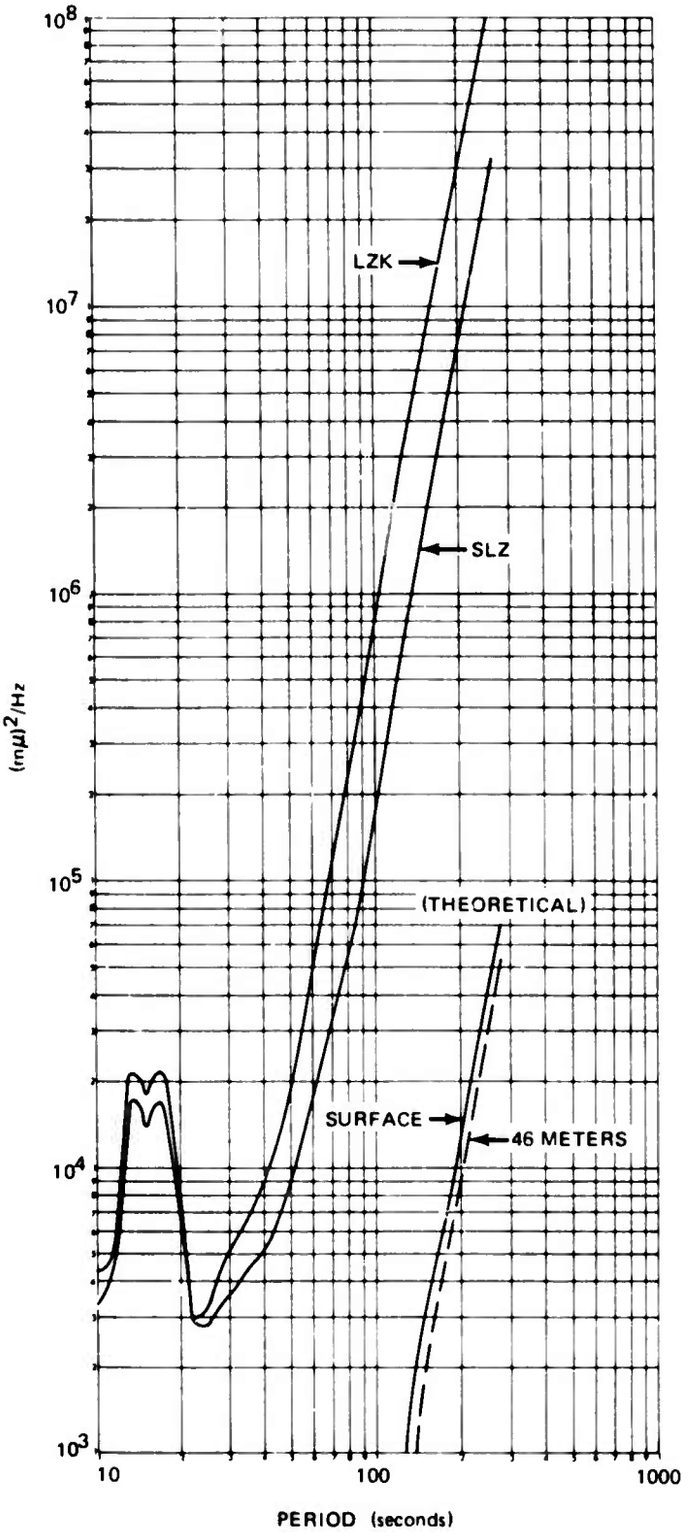

Figure 22. Power spectra of the noise recorded by vertical seismographs at 46 m (SLZ) and the surface (LZK). Wind velocity 5 m/sec. Also shown is theoretically predicted noise corrected for seismograph response, Pinedale, Wyoming.

G 8364

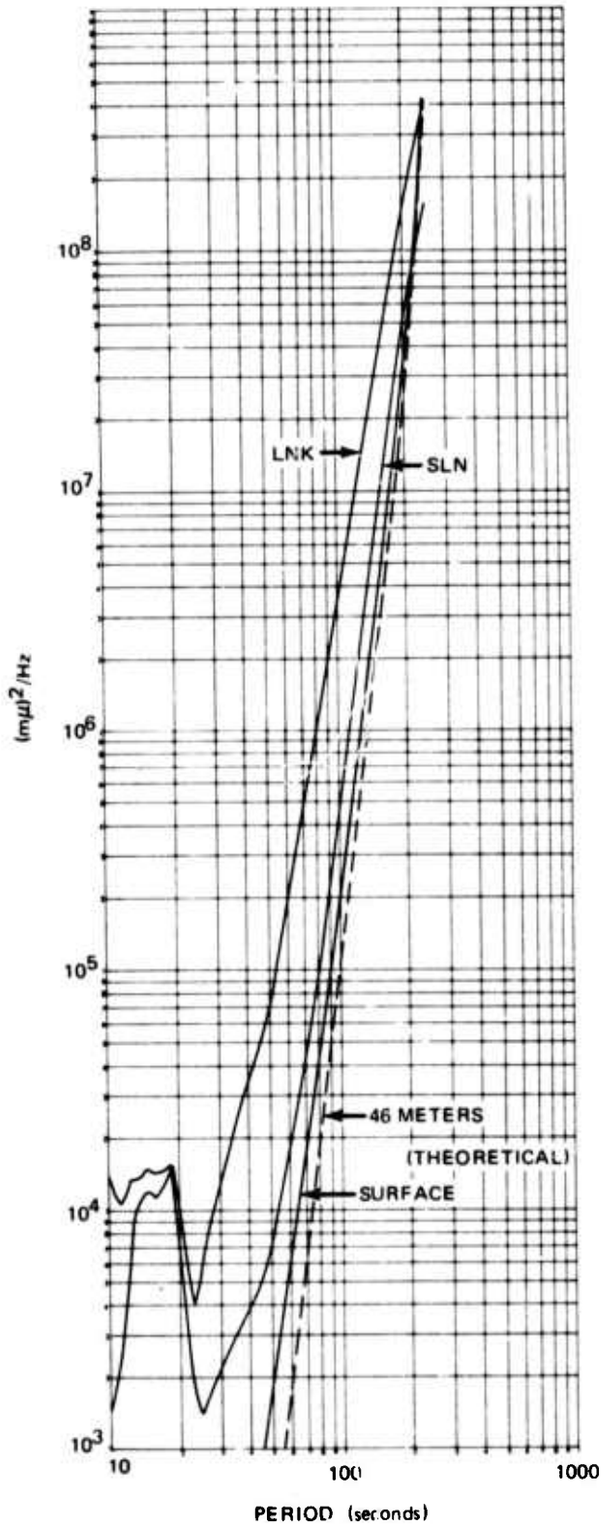

Figure 23. Power spectra of the noise recorded by horizontal seismographs at 46 m and at the surface. Wind velocity 5 m/sec. Also shown is theoretically predicted noise. Corrected for seismograph response, Pinedale, Wyoming.

G 8365

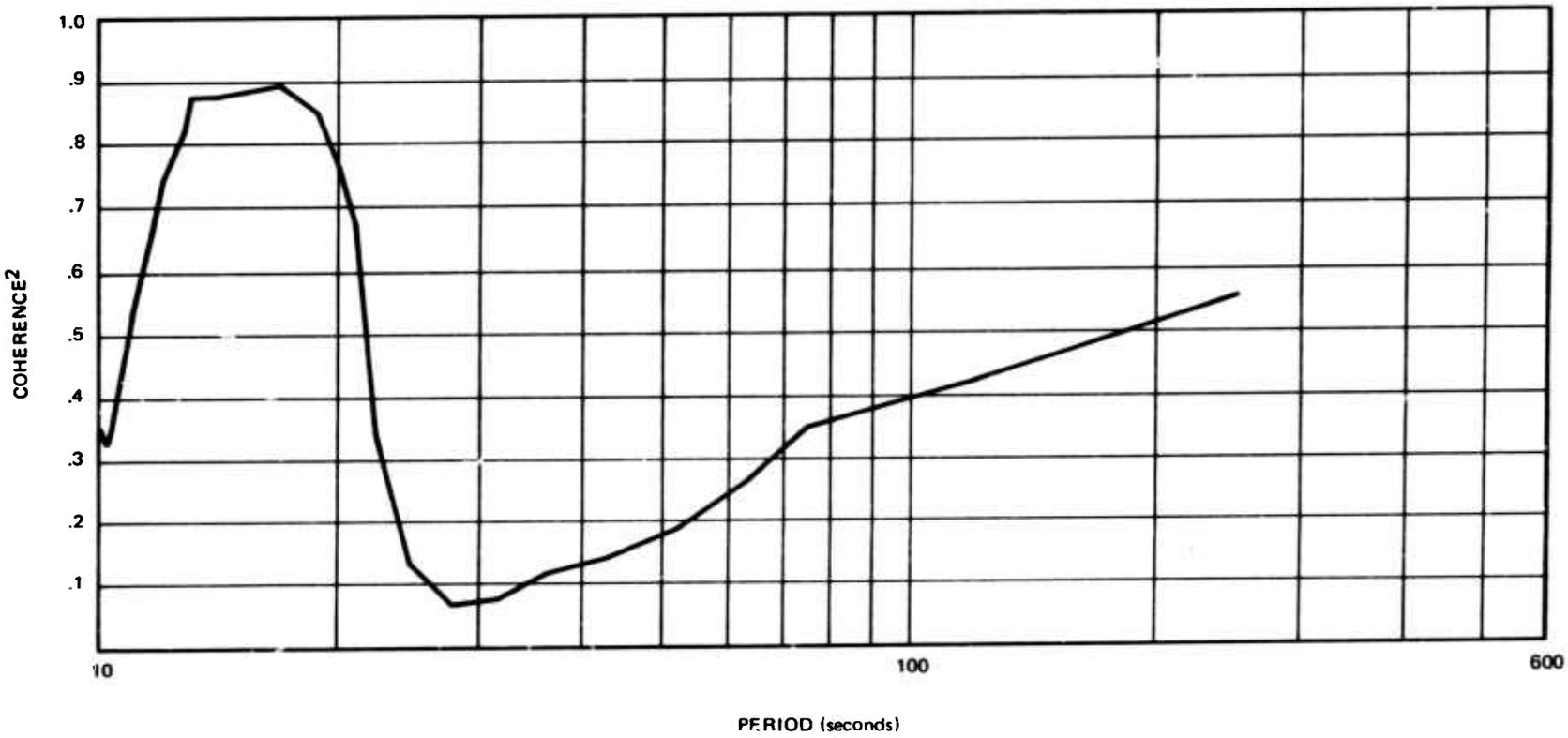

Figure 24. Coherence between recordings from vertical seismographs at depth of 46 m and at the surface.

G 8366

7. CONCLUSIONS

The main source of noise that affects surface seismographs in the period range of 20-100 seconds is the pressure variation caused by wind-generated turbulence. The principal proof consists of the high coherence between seismographs and colocated microbarographs. Environmental effects are also present and are especially severe on long-period horizontal seismographs because of their tilt sensitivity.

The sources of the noise during windless days or at depth are not well established. Both seismic waves and atmospheric pressure variations appear to contribute to the noise levels. Acoustic waves in the atmosphere are the main contributor and are the principal reason for the seasonal variations in the otherwise stable noise spectrum.

Of the two methods of suppressing wind-generated noise, burial at depth and prediction filtering, the former is the more effective. At depths at which the wind-generated noise is eliminated (approximately 50 m in hard rock) both horizontal and vertical seismographs have low noise levels. No further reduction is obtained by installing seismographs at greater depths than that required to eliminate the short wavelength pressure variations associated with the wind. Prediction filters using colocated microbarographs to predict and thus eliminate the wind-generated noise recorded by surface seismographs are very effective when applied to vertical seismographs. For horizontals the results are variable and prediction does not result in appreciable noise reduction.

8. REFERENCES

Anderson, O. L., and Lieberman, R. C., 1966, Sound velocities in rocks and minerals, VESIAC Report 7885-4-X, Willow Run Lab., University of Michigan

Bendat, J. S., and A. G. Piersol, 1968, Measurement and Analysis of Random Date, Wiley, New York, 390 p.

Burg, J. P., 1964, Three-dimensional filtering with an array of seismometers: Geophysics, 29, p. 693-713.

Capon, J., (1969), Investigation of long-period noise at the large aperture array, J. Geophys. Res. 74, 3182-3194.

Cooley, J. S., and Tukey, J. W., 1965, An algorithm for the machine computation of complex Fourier series: Math. Comput. 19, p. 297-301.

Crary, A. P., and Ewing, M., 1952, On a barometric disturbance recorded on a long-period seismograph, Trans. Am. Geoph. Union, 33, 499-502.

Douze, E. J., and Sherwin, J. R., 1975, Deep borehole operation of the Borehole Seismometer System, Model 36000, Tech. Report No. 75-2, Teledyne Geotech, 82 p.

Douze, E. J. and G. G. Sorrells (1974) Prediction of wind related earth noise Bull. Seis. Soc. Am., 65, 637-650.

Douze, E. J. and Starkey, 1973, Evaluation test on KS Seismometer, Tech. Note No. 6-73, Teledyne Geotech, 16 p.

Fix, J.E., 1972, Theoretical and observed noise on a high sensitivity long-period seismograph.

Herrin, E. and McDonald, 1971, A digital system for the acquisition and processing of geoacoustic data: Geoph. J., 26, p. 13-20.

Holcomb, J.G., 1975, Borehole evaluation of the Teledyne Geotech 36000 Seismometer system at Albuquerque, New Mexico, U.S.G.S. Open File Report

Levinson, N., 1949, The Wiener rms error criterion in filter design and prediction; Appendix B of Wiener, N., 1949, Extrapolation interpolation, and smoothing of stationary time series: Wiley, New York.

Lumley, J. L. and H. L. Panofsky (1964), The Structure of Atmospheric Turbulence, Wiley, New York, 239 p.

Melton, B. S., 1975, The sensitivity and dynamic range of inertial seismographs, submitted to Rev. Geoph.

Nur, Amos, Viscous phase in rocks and the low-velocity zone, Jour. Geophys. Res., 76, 1270, 1971.

Robinson, E. A., 1967, Multichannel time series analysis with digital computer programs: Holden-Day, 298 p.

Sacks, I. S., Evertson, D., and Dorman, L. M., 1970, Borehole strainmeters: Carnegie Institution Yearbook, Dept. of Terrestrial Magnetism, p. 426-427.

Savino, J., 1971, The nature of long-period (20 to 130 sec) earth noise and importance of a pronounced noise minimum to detection of seismic events, PL. D. Thesis, Columbia, University.

Savino, J., K. McKamy, and G. Hade, 1972, Structures in earth noise beyond 20 seconds: a window for earthquakes, Bull. Seis. Soc. Am. 62, 141-176 p.

Smart, E., and Flinn, E. A., 1971, Fast frequency wave number analysis and Fisher signal detection in real-time infrasonic array data processing, Geoph. J. 26, 279-284 p.

Sorrells, G. G., 1971, A preliminary investigation into the relationship between long-period seismic noise and local fluctuations in the atmospheric pressure field, Geophys. J. 26, 71-82 p.

Sorrells, G. G., J. A. McDonald, Z. A. Der, and E. Herrin, 1971, Earth motion caused by local atmospheric pressure changes, Geophys. J. 26, p. 83-98.

Sorrells, G. G., and T. T. Goforth, 1973, Low frequency earth motion generated by slowly propagating, partially organized pressure fields, Bull. Seis. Soc. Am. 63, p. 1583-1601.

Sorrells, G. G. and E. J. Douze, 1974, A preliminary report on infrasonic waves as a source of long-period seismic noise, J.Geophys. Res., 79 p. 4908-4917.

Starkey, O. D., 1973, Design and performance of a three-component long-period seismometer system for use in boreholes: Presented at the 17th Gen. Assoc. I.U.C.C., Lima, Peru.

Welch, P. D., 1967, The use of Fast Fourier transforms for the estimation of power spectra: Trans. IEEE AU-15, p. 70-73.

White, R. E., 1973, The estimation of spectra and related quantities by means of multiple coherence function: Geoph. Prosp. 21, p. 660-703.

Ziolkowski, Anton, 1973, Prediction and suppression of long-period non-propagating seismic noise, Bull. Seis. Soc. 63, p. 937-958.

APPENDIX to TECHNICAL REPORT 75-14

CONVECTION IN BOREHOLES

CONVECTION IN BOREHOLES

During the course of operating long-period seismographs in boreholes, it was found that convection currents in the fluid in the casing can seriously affect the performance of the system. The convection currents are caused by temperature gradients. Hales (1937) derived a formula for the instability threshold for positive geothermal gradients:

$$\left(\frac{\Delta T}{\Delta z}\right)_{\text{critical}} = \frac{g\alpha T}{C_p} + \frac{B\nu k}{g\alpha a^4}$$

Here

g	= accel. of gravity	B	= 216 (constant)
α	= coeff. of expansion	ν	= kinematic visosity
T	= absolute temp.	k	= thermal diffusivity
C_p	= specific heat	a	= radius of hole.

The first term of this formula is the adiabatic gradient of the fluid (10°C/km for dry air and 0.2°C for water at 20°C). The geothermal gradient in the earth is generally greater than 10°C/km; hence, stability or instability will depend mostly upon the second term, which is strongly dependent on the hole radius and less so upon the thermal properties of the fluid. Diment (1967) shows that the fluid in nearly all deep wells should be unstable. Indeed, he measured continual temperature fluctuations up to 0.05°C in amplitude and between 1 and 50 minutes in period at most depths in such a well filled with water. (His instruments were incapable of following fluctuations of shorter periods.) Gretener (1967) obtained similar results. Both of these workers found indications that the convection eddies believed to exist were comparable to the hole diameter in vertical extent. Both Gretener (1967) and Garland and Lennox (1962) showed that the observed thermal instabilities could be stopped by reducing the hole diameter by means of a cemented-in inner casing or a loose bundle of tubes. The critical diameter corresponded in order of magnitude to that predicted by Hales' formula.

In two instances the performance of long-period seismographs was seriously degraded by convection currents. The first case occurred at the Alaskan Long-Period Array; at this site triaxial long-period seismographs were installed in 13 in. casings.

During the winter months the noise level of the seismographs increased appreciably. After much experimentation the noise was found to be caused by intense convection currents in the top few feet of the casing. During the winter a very high positive temperature gradient can be expected because of the sub-zero weather. A microbarograph measuring pressure variations inside

the casing recorded pressure variations of 100 $\mu bar^2/Hz$ at 60-second period; this is approximately equivalent to the pressure variations that occur in the atmosphere when the wind is blowing at 5 m/sec.

During operation of the KS seismographs, one of the most prominent features on the recordings were oscillations at periods greater than 60 seconds when the instrument was in the water-filled part of the hole. Using Hale's (1937) formula the following critical gradients were computed.

The effect of various fluids is summarized for the large diameter section of the Pinedale well in the following table of calculated critical thermal gradients, after Hales (1937).

	8.92 in. diameter borehole	
Hole fluid:	Air	Water
Critical temperature gradient, deg C/meter:	0.0164	0.0003

The geothermal gradient in the well is approximately .01°C/m, from a temperature log table when the well was first drilled. Thus, the geothermal gradient suggests that the water column is unstable while the casing filled with air is stable. However, the down-hole electronics dissipates heat, thus the stability of the air column cannot be taken for granted. The spectra of the noise taken for the seismographs operating in air-filled casing do not indicate the presence of convections of sufficient magnitude, if any, to effect the performance of the seismographs.

Figure 20 in the body of the report shows the power spectra of the noise recorded by the east components of the shallow- and deep-hole seismographs. The deep-hole instrument was at 914 m in the water-filled portion of the hole. The long-period noise that is being attributed to convection currents is clearly noticeable for periods greater than approximately 40 seconds, and the power level increases rapidly towards the longer periods. A comparison with the spectra from the deep-hole verticals shows that the long-period oscillations are not present on the vertical component. Therefore, this type of noise is almost certainly caused by tilting of the instrument package.

REFERENCES

Diment, W. A., 1967, Thermal regime of a large diameter borehole: geophysics, J32, p. 720-726.

Garland, G. D., Lennox, D. H., 1962, Heat flow in Western Canada: geoph. J., v. 6, p. 245-261.

Gretener, P. E., 1967, On the thermal instability of large diameter wells: geophysics, J32, p. 720-726.

Hales, A. L., 1937, Convection currents in geysers: Monthyl Notes, Royal Astr. Soc. geoph. Suppl., J4, P. 122-131.